

**Admixture affects the rate and repeatability of experimental adaptation to a stressful environment in *Callosobruchus maculatus***

**Amy Springer<sup>1</sup>, Brian Kissmer<sup>2,3</sup>, Zachariah Gompert<sup>2,3</sup>**

<sup>1</sup> College of Natural Resources, University of Wisconsin-Stevens Point, Stevens Point, WI 54481, USA

<sup>2</sup> Department of Biology, Utah State University, Logan, UT 84322, USA

<sup>3</sup> Ecology Center, Utah State University, Logan, UT 84322, USA

Send correspondence to:

aspringe@uwsp.edu and zach.gompert@usu.edu

# Abstract

Admixture is common in nature, and can serve as a crucial source of adaptive potential through the generation of novel genotype combinations and phenotypes. Conversely, the presence of hybrid incompatibilities can decrease the fitness of hybrids. Due to the pervasiveness of admixture in nature and its potential role in facilitating adaptation, understanding how admixture affects the rate and repeatability of evolution is important for furthering our understanding of evolutionary dynamics. However, few studies have assessed how patterns of evolutionary parallelism in admixed lineages are affected by the presence of strong ecological pressure. In this experiment, we assessed patterns of evolution and parallelism across admixed and non-admixed cowpea seed beetles (*Callosobruchus maculatus*) during adaptation to a novel, stressful host: lentil. Specifically, we asked (1) whether admixture facilitates adaptation to lentil, (2) whether parallelism was higher in admixed or non-admixed lineages, and (3) to what degree parallelism in admixed lineages was associated with selection on globally adaptive alleles versus epistatic effects and hybrid incompatibilities. We found that admixture facilitated adaptation to lentil, and evolutionary rescue—defined as adaptation that prevents population extinction—occurred in all lineages. The degree of evolutionary parallelism was highest in two admixed lineages, but notable in all lineages. Adaptation to lentil appeared to be driven by selection on alleles that were globally adaptive. However, even during evolutionary rescue in a marginal environment, the purging of hybrid incompatibilities appeared to contribute substantially to evolutionary parallelism in admixed lineages.

**Keywords:** *Callosobruchus maculatus*, adaptation, parallel evolution, Bayesian linear models, admixture, evolutionary rescue

## 23 Introduction

24 Admixture is increasingly being recognized as a major driver of evolutionary dynamics, as  
 25 well as a potentially critical source of adaptive potential. Admixture is a widespread phe-  
 26 nomenon, occurring in at least 10% of animal and 25% of plant species (Mallet, 2005), and a  
 27 substantial portion of many species' genomes—including our own—are derived from hybrid  
 28 origins (Gompert *et al.*, 2006; Hermansen *et al.*, 2011; Edwards *et al.*, 2011; Sankararaman  
 29 *et al.*, 2016; Schumer *et al.*, 2016; Meier *et al.*, 2017; Short & Streisfeld, 2023; Rosser *et al.*,  
 30 2024). Admixture events can result in the transfer of just a few alleles from one population  
 31 to another (i.e. adaptive introgression) (Enard & Petrov, 2018; Oziolor *et al.*, 2019; Nanaei  
 32 *et al.*, 2023; Rossi *et al.*, 2024), the reinforcement of species boundaries (Bewick & Dyer, 2014;  
 33 Turissini & Matute, 2017; Bhargav *et al.*, 2022), or in some cases, genome stabilization and  
 34 the formation of stable mosaic hybrid species (Gompert *et al.*, 2006; Mallet, 2007; Schumer  
 35 *et al.*, 2018; Sun *et al.*, 2020; Rosser *et al.*, 2024). By bringing together new combinations  
 36 of alleles from previously isolated parental populations, admixture can create novel pheno-  
 37 typic variation (i.e. transgressive segregation) and serve as a source of evolutionary novelty  
 38 (Lewontin & Birch, 1966; Rieseberg *et al.*, 1999; Pereira *et al.*, 2014; Chhina *et al.*, 2022).  
 39 The extreme phenotypes generated by admixture combined with the transfer of globally  
 40 beneficial alleles (i.e. adaptive introgression) and the genetic benefits of outbreeding (e.g.,  
 41 heterosis and the masking of deleterious recessive alleles) can increase the adaptive potential  
 42 of admixed populations, particularly in novel or marginal environments (Crow, 1948; Buerkle  
 43 *et al.*, 2000; Gompert *et al.*, 2006; De Carvalho *et al.*, 2010; Oziolor *et al.*, 2019; Durkee *et al.*,  
 44 2023). Conversely, the presence of Dobzhansky-Muller incompatibilities (Dobzhansky, 1982)  
 45 and the breakdown of adaptive gene complexes can reduce fitness in admixed individuals  
 46 (i.e. outbreeding depression), leading to selective pressure against hybridization (Verhoeven  
 47 *et al.*, 2011; Turissini & Matute, 2017; Kim *et al.*, 2018; Calvo-Baltanás *et al.*, 2021; Bhargav  
 48 *et al.*, 2022; Mantel & Sweigart, 2024). Because admixed populations are subject to multiple  
 49 conflicting evolutionary pressures, the evolutionary outcomes of admixture vary widely. As

such, determining the degree to which evolution in admixed populations is repeatable—and therefore predictable—is of particular interest for understanding how deterministic processes (e.g., natural selection imposed by the environment) and constraints imposed by admixture interact to shape patterns of genomic change.

The degree of repeatability in genome evolution post-admixture depends on many factors, including demographic history, the degree of genetic divergence between parental populations, recombination landscapes across the genome, and how far from the phenotypic optimum each parental population is in the environment where admixture occurs (Schumer *et al.*, 2018; Moran *et al.*, 2021; McFarlane *et al.*, 2022; Langdon *et al.*, 2024; Owens *et al.*, 2025). A few general principles have already emerged regarding the repeatability of evolution at a genomic level post-admixture, including the purging of ancestry derived from the minor parental population—the parental population that contributed the least amount of ancestry to the hybrid genome (Schumer *et al.*, 2018; Chaturvedi *et al.*, 2020; Moran *et al.*, 2021; Langdon *et al.*, 2022, 2024). When Dobzhansky-Muller incompatibilities are present or intermediate hybrid phenotypes are ecologically unsuitable for the environment, purging ancestry from the minor parent can be the most direct evolutionary route for adaptation in admixed populations (Langdon *et al.*, 2022). Purging of minor parent ancestry may even be repeatable across hybrids formed from different species pairs (Langdon *et al.*, 2022, 2024). Similarly, when one parental population has a lower effective population size than the other (i.e. island versus mainland populations, see Matute *et al.*, 2020), mildly deleterious alleles that accumulated and fixed in the smaller population via genetic drift can result in strong selection against ancestry from that population (Harris & Nielsen, 2016; Juric *et al.*, 2016). Selective pressure against this hybridization load can lead to purging of entire blocks of local ancestry inherited from the smaller, more inbred population, especially at sites with low recombination rates (Matute *et al.*, 2020; Nouhaud *et al.*, 2022).

However, while a considerable amount of work has been done to determine factors shaping the repeatability of evolution in admixed populations in an organism’s native habi-

tat (Rieseberg *et al.*, 2003; Schumer *et al.*, 2018; Chaturvedi *et al.*, 2020; Langdon *et al.*,  
 2022; Nouhaud *et al.*, 2022; Langdon *et al.*, 2024; Owens *et al.*, 2025) or under benign lab-  
 oratory conditions (Matute *et al.*, 2020), few studies explicitly address the impact of strong  
 directional selection imposed by stressful ecological conditions on patterns of evolutionary  
 repeatability in admixed populations. Given the strong potential for admixture to facil-  
 itate adaptation and evolutionary rescue—defined as adaptation that prevents population  
 extinction—under stressful environmental conditions via the expression of transgressive phe-  
 notypes and transfer of globally adaptive alleles (Lewontin & Birch, 1966; Gompert *et al.*,  
 2006; De Carvalho *et al.*, 2010; Pereira *et al.*, 2014; Stelkens *et al.*, 2014; Oziolor *et al.*, 2019;  
 Vedder *et al.*, 2022; Durkee *et al.*, 2023), this remains a critical gap in our understanding  
 of the predictability and repeatability of evolution in admixed populations. In the face of  
 unprecedented anthropogenic change, determining how strong ecological selection alters the  
 genomic consequences of admixture is also of critical relevance for determining the effect of  
 admixture on adaptive potential. While intrinsic hybrid incompatibilities commonly drive  
 patterns of repeatability during the evolution of admixed populations (Chaturvedi *et al.*,  
 2020; Matute *et al.*, 2020; Langdon *et al.*, 2022; Nouhaud *et al.*, 2022; Owens *et al.*, 2025),  
 the severe population bottlenecks that occur during evolutionary rescue could drastically  
 increase the degree of stochasticity experienced during adaptation, potentially reducing re-  
 peatability (see McFarlane *et al.*, 2022). Conversely, when populations begin far from the  
 phenotypic optimum, rapid adaptation during evolutionary rescue may be initially driven  
 by selection of just a few major-effect loci (rather than many small-effect loci) (Orr, 2005;  
 Alexander *et al.*, 2014). Selection concentrated on a few loci during bouts of rapid adapta-  
 tion could potentially increase the repeatability of evolution during evolutionary rescue, but  
 how the influx of novel standing genetic variation plus intrinsic incompatibilities introduced  
 via admixture might alter patterns of selection and change during evolutionary rescue is  
 unclear.

In this study, we used experimental evolution to assess how admixture affects pat-

terns of evolutionary rescue and repeatability in cowpea seed beetles, *Callosobruchus mac-*  
*ulatus*, during adaptation to a novel, stressful host. *Callosobruchus maculatus* is a globally-  
distributed pest of stored legumes from the tribe Phaseoleae (e.g., mung bean, adzuki bean,  
and cowpea; Tuda *et al.*, 2006; Kéb   *et al.*, 2017). Because cowpea seed beetles have been  
associated with human crop stores for thousands of years and their larvae spend the en-  
tirety of their development within a single seed, laboratory conditions closely approximate  
the “natural” habitat of *C. maculatus* (Messina, 1991; Tuda *et al.*, 2014; K     *et al.*, 2017).  
Populations from different geographic locations vary substantially in fitness traits, including  
larval competitiveness, body size, oviposition preference, and fecundity (Credland & Dick,  
1987; Messina, 1991, 1993; Messina *et al.*, 2018; Burc *et al.*, 2025). Lentil (*Lens culinaris*,  
tribe Fabeae) is a particularly poor host for *C. maculatus* (Messina *et al.*, 2009). Initial  
survival on lentil is often less than 3%, and experimental attempts to establish *C. maculatus*  
populations on lentil sometimes result in extinction (Messina *et al.*, 2009, 2020). Despite  
this, *C. maculatus* lineages on lentil that do not go extinct have been found to rapidly re-  
bound, with percent survival rising to over 80% within 20 generations (Messina *et al.*, 2009;  
R     *et al.*, 2019). Previous ecological studies have shown that admixture likely facilitates  
adaptation to lentil in the cowpea seed beetle (Messina *et al.*, 2020), and previous genomic  
studies have found a modest degree of parallelism at a genomic level across non-admixed  
lineages during adaptation to lentil (Gompert & Messina, 2016; R     *et al.*, 2019). However,  
to date no studies have assessed how both admixture and environmental stress combined  
affect the repeatability of genomic change during adaptation a novel, stressful host.

Here, we assessed how admixture affects ecological (demographic) and evolutionary  
dynamics and the degree of evolutionary parallelism (repeatability of genomic change) during  
adaptation to lentil in *C. maculatus*. Specifically we asked the following questions: (1) to  
what degree does admixture facilitate adaptation to lentil, (2) is evolution more repeatable  
in admixed or non-admixed lineages during evolutionary rescue, and (3) to what degree is  
repeatability during evolutionary rescue in admixed lineages driven by (a) a shared genetic

basis for adaptation to lentil across admixed and non-admixed lineages (i.e. selection on globally-adaptive alleles where the beneficial effects do not depend on genetic background) versus (b) a shared genetic basis for adaptation in admixed (but not non-admixed) lineages independent of host plant, which would suggest epistatic effects in hybrid lineages and the purging of hybrid incompatibilities?

## Materials and Methods

### Experimental Design

We used cowpea-adapted lineages of *Callosobruchus maculatus* from three different continents for this experiment: Burkina Faso (Africa), Brazil (South America), and California (North America) (Fig. 1). These lineages all originally utilized cowpea, *Vigna unguiculata*, as their native host, have non-competitive larvae, and show low initial survival rates on lentil (Messina *et al.*, 2020). All lineages were obtained from Dr. Charles Fox at the University of Kentucky (Messina *et al.*, 2018), but were originally collected from infested cowpeas in the field or in markets across the world. Cultures from all three lineages were maintained continuously in the laboratory on cowpea after their initial collection. The Burkina Faso (BF) lineage was collected from a field of cowpeas (*V. unguiculata*) in Ouagadougou, Burkina Faso by Dr. J. Huignard at the University of Tours in 1989 (Messina, 1993; Messina *et al.*, 2018). The Brazil population (BZ) was collected from Campinas, Brazil in 1975 (Tran & Credland, 1995) and later maintained by Dr. Robert Smith at the University of Leicester (Guedes *et al.*, 2003; Dowling *et al.*, 2007a). The North American lineage was collected from California (CA) and later maintained by Dr. Peter Credland at the University of London (Tuda *et al.*, 2014; Dowling *et al.*, 2007b). All lineages are estimated to have been maintained under standard laboratory conditions in excess of 300 generations at the time of our experiment.

We began our experiment with a single stock colony each from the BF, BZ, and CA lineages (3 jars total). These colonies had been maintained in the laboratory at Utah State University in excess of 100 generations at the time of this experiment. Colonies were kept in 2 L glass jars containing approximately 750 g of cowpeas. New generations were founded by transferring ~2000 newly-emerged adult beetles (estimated by volume using an insect aspirator) to fresh culture jars once every 25-30 days (hereafter referred to as “standard culture”). During this experiment, all colonies were housed at 27°C with a 14/10 day cycle in one of two Percival incubators (both model No. I-36VL). Due to the large amount of metabolic water produced by growing beetle larvae, we installed a dehumidifier in each incubator to reduce humidity levels to between 15-50%. While under standard culture conditions only 2000 adult beetles per generation are transferred, each jar will produce far more than 2000 adult beetles each generation. This allows us to split any given jar of beetles into multiple daughter colonies each month without imposing a population bottleneck on the original colony. To found the colonies for our experiment, each month from our stock colonies we removed (1) 2000 adult beetles to found the next generation of the stock colony, (2) 2000 adult beetles to found the purebred control colonies for that month’s replicates, and (3) approximately 1000 pupae-containing beans to use for that month’s admixed replicates.

To form our admixed lineages, we produced true F1 hybrids with a founding population size of 1000 parental beetles each. To accomplish this, one to three days before the beetles’ expected emergence date, we randomly sampled 1000 pupae-containing beans from each of our parental stock colonies. These beans were isolated in individual cellulose pill capsules and maintained in the incubator under standard conditions. Twice daily, emerging virgin beetles were tallied and sorted into petri dishes by population and sex. This process was continued until we had collected four dishes of 250 virgin beetles each from each stock colony: two all-male and two all-female dishes from each parental population (BF, BZ, and CA). Reciprocal crosses were then performed for each combination of parental populations. In other words, we placed 250 virgin males from the first parental population in a jar with



250 virgin females from the second, and vice versa in a second jar. After 10 days (at which point most or all of the purebred adults had died), we combined each male×female jar with its reciprocal female×male pair to found a single admixed colony comprised of the true F1 offspring of the 1000 purebred founding beetles. This method ensured we were producing admixed lineages with equal genetic contribution from both sexes from each parental populations. To found our purebred control colonies, we simply transferred 1000 beetles (as measured by volume) from each purebred stock colony to fresh culture jars. We produced 11 full replicates, where each replicate consisted of three purebred (BF, BZ, CA) and three admixed (BF×BZ, BF×CA, BZ×CA) cowpea colonies each, for a total of 66 cowpea colonies with a founding population size of 1000 beetles per jar (Fig. 1).

After maintaining both our purebred and admixed colonies on their native host (cowpea) for two successive generations post-admixture, we split each of our 66 cowpea colonies to form 66 additional colonies on our novel, stressful host: lentil. To do so, we removed a total of 4000 adult beetles (as measured by volume) from each of our 66 F2 cowpea colonies and transferred 2000 to fresh lentil culture jars and 2000 to fresh cowpea culture jars to lay eggs. Thus, the first generation of beetle larvae to feed on the novel food source in our experiment was the F3 generation. This left us with a total of 132 beetle colonies and 12 (replicated) lineages: three admixed and three non-admixed lineages on cowpea, and three admixed and three non-admixed lineages on lentil. This full factorial experimental design allowed us to compare the evolution and performance of admixed lineages across environments (stressful versus benign), as well as compare evolution and performance of admixed versus purebred lineages within each of those environments. We chose not to conduct the host shift onto lentil until the F2 generation because F1 hybrids are typically phenotypically uniform and thus will not reflect the adaptive potential that could emerge after independent assortment and recombination break down ancestry blocks generating novel genotypic combinations (i.e. transgressive segregation). All 132 colonies were maintained for at least 20 generations post-admixture (at least 17 generations post-host shift). After this time colonies were culled via

209 freezing.

## 210 **Population Growth Assays**

211 During the first 400 days after the host shift onto lentil (or until enough beetles emerged  
 212 to move the colony into standard culture), we removed all dead adult beetles produced by  
 213 each of the 66 lentil colonies. This was done to assess the rate of adaptation to lentil in each  
 214 colony, measured by population growth. Every 20 days, beetles from each lentil colony were  
 215 separated from the beans using a soil sieve. All live beetles were aspirated from the upper  
 216 edge of the sieve and returned to the culture jar to continue laying eggs. This was done to  
 217 ensure that population sizes during adaptation to lentil were not altered by our population  
 218 growth tracking method. All dead beetles remaining at the bottom of the sieve were removed  
 219 and stored at -80°C until image analysis. Thus, each sample of beetles removed represents  
 220 the number of adult beetles that died during the previous 20-day period, and the full set  
 221 of such samples for each colony provides an accurate estimate of the cumulative population  
 222 size of each colony over time.

223 To assess the number of adult beetles produced by each colony during every 20 days  
 224 post host-shift, we used the program **ImageJ** (version 1.52A) (Schneider *et al.*, 2012). Beetle  
 225 specimens from each sample were photographed using a Canon EOS M6 camera. Pho-  
 226 tographs were first prepared for analysis using the program Adobe Photoshop Elements  
 227 2020 Editor to correct uneven lighting and ensure the background color was uniform across  
 228 the entire image. This was necessary to ensure that **ImageJ** could accurately differenti-  
 229 ate between the color of beetles versus the background sheet. We then used the **analyze**  
 230 **particles** function in ImageJ to count the number of beetles in each image. The result  
 231 of this analysis was a count of the total number of beetles that died during every 20-day  
 232 period in each colony post host-shift. As we collected every dead beetle produced by each  
 233 jar during each 20 day interval between 60 and 400 days post host shift (unless the colony  
 234 was moved into standard culture prior to 400 days post host shift), these population counts

represent a complete count of the total number of beetles produced by each colony during early adaptation to lentil.

We analyzed population growth in both admixed and non-admixed lines using a Bayesian generalized linear model. Cumulative count data were assumed to follow a normal distribution with  $\mu = \mu^{count}$  and  $\sigma = \sigma^{count}$ . Mean cumulative population count ( $\mu^{count}$ ) was assumed to follow a second order polynomial relationship with respect to the number of days post host shift such that for non-admixed lineages:

$$\mu^{count} = (\beta_1^{pop} + \alpha_1^{rep})days + (\beta_2^{pop} + \alpha_2^{rep})days^2$$

where  $\beta_1^{pop}$  and  $\beta_2^{pop}$  are the effects of time (calculated as the standardized but not centered number of days post host-shift) on the mean cumulative number of beetles that emerged for each non-admixed population, *pop* is the particular non-admixed population being considered (BF, BZ, or CA), *days* is the number of days post host-shift, and  $\alpha_1^{rep}$  and  $\alpha_2^{rep}$  are random effects of replicate for each  $\beta$ -term (data from replicates 2 through 10 were used for this analysis). Replicate effects were transformed with a sum-to-zero constraint to ensure all parameters in the model were identifiable. For admixed lineages,  $\mu^{count}$  was assumed to follow the same polynomial relationship shown above except that each slope ( $\beta_1$  and  $\beta_2$ ) for admixed populations was assumed to equal the average slope from each parental lineage plus an additional effect of admixture, such that:

$$\mu_{count} = \left( \frac{\beta_1^{P1} + \beta_1^{P2}}{2} + \beta_1^{AE} + \alpha_1^{rep} \right) days + \left( \frac{\beta_2^{P1} + \beta_2^{P2}}{2} + \beta_2^{AE} + \alpha_2^{rep} \right) days^2$$

where  $\beta^{P1}$  terms are the effects of time on cumulative beetles emerged in the first parental lineage,  $\beta^{P2}$  terms are the effects of time on cumulative beetles emerged in the second parental lineage, and  $\beta^{AE}$  terms are the additional effects of admixture on the cumulative

beetles emerged. Thus, our model included six  $\beta_1$  and six  $\beta_2$  parameters (one slope parameter for each of the three parental lineages, and one admixture effect parameter for each of the three admixed lineages). Both the  $\beta_1$  and  $\beta_2$  parameters were assigned a normal prior with  $\mu = 0$  and  $\sigma = 100$ . Raw (not sum-to-zero transformed) random replicate effects (i.e.  $\alpha_1$  and  $\alpha_2$  parameters) were assigned normal priors with  $\mu = 0$  and  $\sigma = \sigma_1^\alpha$  and  $\sigma_2^\alpha$  respectively. Finally, all three sigma parameters ( $\sigma^{count}$ ,  $\sigma_1^\alpha$ , and  $\sigma_2^\alpha$ ) were assigned gamma priors with parameters  $k = 0.1$  and  $\theta = 0.01$ . This model was written in the language Stan (Stan Development Team, 2022b) and implemented with the R-interface `rstan` version 2.21.5 (Stan Development Team, 2022a). We ran 5 chains with a burn-in period of 1,500 steps and 3,000 Hamiltonian Monte Carlo (HMC) sampling steps.

## DNA Sequencing, Alignment, and Variant Calling

We extracted DNA from between 19-20 beetle specimens each from 78 unique lineage, replicate, host and generation combinations, for a total of 1536 individuals (Fig. 1). As cowpea seed beetles have an XY sex chromosome system and the Y-chromosome is significantly reduced in size (Angus *et al.*, 2011; Arnqvist *et al.*, 2023), we chose to sequence only female beetles to achieve better coverage of the X-chromosome. We sequenced DNA from three time points during our experiment: generation 1 (F1; pre-adaptation), generation 7 (F7; early adaptation), and generation 20 (F20; late adaptation). From the F1 generation, we sequenced only purebred parental cowpea lineages (BF, BZ, and CA) from replicate 1. Because our admixed lineages were true F1 hybrids of our parental cowpea lineages, the initial allele frequencies of our first generation hybrid lines could be inferred from the allele frequencies of these original parental lines. From the early adaptation (F7) generation we sequenced replicates 1 to 5 for all cowpea- and lentil-adapted admixed lineages (BF $\times$ BZ, BF $\times$ CA, and BZ $\times$ CA) for a total of 30-F7 experimental groups. From our late adaptation time point (F20) we again sequenced beetles from replicates 1 to 5 from all admixed lineages (both cowpea- and lentil-adapted), as well as all purebred lentil-adapted populations for a

total of 45-F20 experimental groups. This sampling scheme allowed us to assess evolution in purebred lines during adaptation to lentil, evolution in admixed lineages during early and late adaptation to lentil, as well as evolution during early and late generation admixed lineages not exposed to a novel host.

To extract DNA from beetle specimens, we used Qiagen DNeasy 96 Blood and Tissue Kits. To minimize cross-contamination of DNA, all beetle specimens were washed prior to DNA extraction. Reduced-representation restriction-fragment-based DNA libraries were then prepared from extracted DNA using the genotyping-by-sequencing (GBS) library preparation protocol described in Parchman *et al.* (2012) and Gompert *et al.* (2012) with modifications from Gompert *et al.* (2014). Briefly, whole-genome DNA was first digested with MseI and EcoRI enzymes, then ligated to custom barcode sequences and amplified via PCR. Barcoded and amplified DNA fragments were pooled, purified, and size-selected on a BluePippin. We selected DNA fragments between 250-350 bp for sequencing. Our DNA fragment libraries (four libraries total, each with 384 individuals) were sequenced on an Illumina NovaSeq (one full run per library with SP 100 cycles) by the Genomics Core at the University of Colorado Anschutz Medical Campus.

Sequencing resulted in a total of 4,381,945,291 individual reads. We first filtered each of the Fastq files to remove PhiX sequences. After the removal of PhiX reads, we were left with a total of 3,539,264,296 reads for alignment. Barcode sequences were then removed from the remaining reads using a custom perl script, and each read was tagged with the ID of the beetle from which it came. We aligned DNA reads from our experiment to the *Callosobruchus maculatus* reference genome (NCBI accession number CASHZR020000000) using the `bwa aln` algorithm (Li & Durbin, 2009). For this, we set the maximum number of mismatches allowed per sequence (`-n`) to 5, the seed length (`-l`) to 20, and the maximum mismatches allowed in the seed sequence (`-k`) to 2.

To identify sites with single nucleotide polymorphisms (SNPs), we conducted variant calling using `bcftools` version 1.16 (Li *et al.*, 2009). We used the original consensus caller

(-c) and called only variants for which the posterior probability of the SNP being invariant was less than 0.01 (-p = 0.01). Variable sites were filtered for quality using custom perl scripts. In particular, we retained only variable sites with a phred-scale mapping quality greater than 30, a coverage level equal to or greater than 3072 reads (2× the number of individuals we sequenced), a minimum of 10 reads for the alternative allele (to filter out possible errors in sequencing), and representing 80% or more of the individuals we sequenced. Variable sites with base-quality rank-sum, mapping-quality rank-sum, or read-position rank-sum test *P*-values less than 0.001, 0.0001, and 0.001 respectively were not retained. After this initial filtering step, SNPs with a read depth exceeding 48,000, that is, 3 standard deviations greater than the mean read depth across loci, were also removed. This was done to remove possible paralogs and gene families from our filtered SNP set. Variable sites located less than 2 bps apart were also removed. After quality filtering, we were left with 79,079 SNPs for downstream analysis.

## Population Genetic Analyses

In order to obtain robust genotype estimates and quantify patterns of admixture and global ancestry (i.e. genome-average ancestry), we used the program **entropy** (version 2.0) (Gompert *et al.*, 2014; Shastry *et al.*, 2021). This program is comparable to the admixture model in **structure**, but with the additional feature of accounting for uncertainty in genotypes, which are estimated from genotype likelihoods as part of the analysis. Because our experiment used three known parental populations for the production of admixed lineages, we ran **entropy** only for  $K = 3$  source populations. We ran 20 Markov chain Monte Carlo (MCMC) chains with 2000 burn-in steps and 2500 sampling steps each, a Dirichlet initialization value of 50, and a thinning interval of 5. Ancestry proportion estimates generated by **entropy** were used to determine the degree to which ancestry proportions shifted over time (for example, if ancestry from one parental lineage was selected against due to incompatibilities or ecological selection). We also visualized patterns of genetic structure among our parental and admixed

lineages by conducting a PCA of the Bayesian genotype estimates from **entropy**. This PCA was performed from centered but unscaled genotype estimates using R version 4.2.2 (R Core Team, 2022).

We then used the program **popanc** (version 0.1) to estimate population-level, local ancestry frequencies along chromosomes for each line (Gompert, 2016). This was done to visualize differences in the frequency of ancestry blocks across the genome and among treatment groups. This program uses a continuous correlated beta process model for inferring ancestry, and is particularly well-suited for inferring ancestry in hybrid populations that do not experience ongoing gene flow with parental populations and for which genome stabilization is not yet complete (Gompert & Buerkle, 2013; Gompert, 2016). We ran **popanc** using the genotype estimates from **entropy**. We only included SNPs assigned to one of the ten *C. maculatus* chromosomes (9 autosomes and the X chromosome; 72,583 of the 79,079 SNPs) and for which the absolute difference in initial allele frequencies between parental lineages (BF versus BZ, BF versus CA, or BZ versus CA) was greater than 0.2. This was done to ensure that only the loci that were informative of population ancestry were used for local ancestry analysis. We chose to have **popanc** estimate the scale parameter for the beta process model (-s) and set a uniform prior on this parameter, U(lower = 1, upper = 100,000) (here measured in bps). We set a maximum locus distance (-d) to one Megabase and the maximum number of SNPs per locus (-n) to 15. We ran two MCMC chains for each admixed lineage with each comprising a 10,000 step burn-in and 30,000 sampling steps with a thinning interval (-t) of 5.

To estimate allele frequencies within each unique lineage, replicate, host and generation combination, we used the program **estpEM** (Soria-Carrasco *et al.*, 2014). **estpEM** uses the expectation-maximization algorithm described in Li (2011) and accounts for uncertainty in genotypes during allele frequency estimation. For this analysis, we used a convergence tolerance of 0.001 and allowed for a maximum of 20 iterations. F1 allele frequency estimates from **estpEM** were used to calculate Nei's  $F_{ST}$  between pairs of non-admixed, parental lin-

eages (i.e. BF, BZ, and CA cowpea lineages) in order to determine the degree of genetic differentiation among our parental lineages. We then computed allele frequency change for all of our sequenced experimental groups. Allele frequency change, or  $\Delta p$ , was calculated as  $\Delta p = p_t - p_0$  where  $p_t$  is the frequency of an allele at time point  $t$  (7 or 20) and  $p_0$  is the initial frequencies of allele. Because we formed true F1 hybrids to establish our admixed populations, the initial allele frequencies of our admixed lineages should be a simple average of the allele frequencies of the parent populations. As such, we estimated the allele frequencies of our F1 hybrid lineages by taking the average of the allele frequencies of their parental lineages.

Finally, we used **varne** to estimate the contemporary, variance effective population size ( $N_e$ ) of each colony based on patterns of allele frequency change during the experiment (Jorde & Ryman, 2007; Gompert & Messina, 2016; Rêgo *et al.*, 2019). This allowed us to (i) estimate the severity of population bottlenecks experienced by both admixed and non-admixed lines during adaptation and (ii) obtain estimates of  $N_e$  to parameterize the null model of expected evolutionary change by genetic drift described in the next section. We estimated variance  $N_e$  between generation F1 and generation F20, and conducted all **varne** analyses with an approximate census size (**-n**) of 2000 beetles and 1000 Bayesian bootstrap replicates (**-x**).

## Testing for Repeated Adaptive Evolution

We constructed a null model to determine whether the observed degree of allele frequency change for each locus in each line was greater than expected by genetic drift alone. We modeled evolution by drift using a beta-distribution approximation to a Wright-Fisher model (Ewens & Ewens, 2004; Gaggiotti & Foll, 2010; Rêgo *et al.*, 2019). Here, the the probability of allele frequency  $p_t$  at time  $t$  follows a beta distribution with  $\alpha = p_0 * (1 - F)/F$  and  $\beta = (1 - p_0) * (1 - F)/F$ , where  $F = 1 - (1 - \frac{1}{2N_e})^t$ . Thus, the magnitude of change by drift depends on effective population size, time, and initial allele frequency. We parameterized the null



model using the actual number of elapsed generations ( $t$ ), our estimates of variance effective population size ( $N_e$ ) from `varne`, and our maximum likelihood estimates of allele frequencies ( $p_0$ ). We constrained allele frequencies to be between 0.01 and 0.99 for numerical stability; greater precision than this would also be difficult to justify from our sample sizes. We converted the one-tailed probability from the beta probability distribution function (`pbeta` in R) to a two-tailed  $P$ -value by taking  $\min[P_{\text{beta}} * 2, (1 - P_{\text{beta}}) * 2]$ . We interpret these  $P$ -values as measures of the evidence against the null hypothesis that evolution occurred only by drift, and thus as evidence that evolution was directly or (more likely) indirectly (via linkage disequilibrium) effected by selection.

We conducted a series of analyses to quantify the extent to which the same loci exhibited the greatest evidence of non-neutral evolution (as captured by our null-model  $P$ -values) (i) across replicate lines of the same lineage and treatment and (ii) between different pairs of lineages or treatments. Thus, we were interested in both whether evolutionary change during adaptation was more repeatable under some conditions than others and whether evolution was more repeatable for certain pairs of conditions (e.g., admixed and non-admixed lines adapting to the same host or admixed lines adapting to different hosts) than others. We first used the program `picmin` to test for repeated, non-neutral evolution at the SNP level for each treatment and sequenced time point (Booker *et al.*, 2023). This approach works by identifying loci (here SNPs) that consistently fall in the tails of an empirical  $P$ -value distribution across a set of populations or species. Such patterns are indicative of a repeated association with adaptation. Most applications of this method have considered somewhat distantly related taxa and have taken gene or window-based approaches (e.g., Nocchi *et al.*, 2024; Whiting *et al.*, 2024). Here, we apply this to replicates of the same source population and focus on individual SNPs (which are necessarily shared across the set of replicates).

For these analyses, we converted the null-model  $P$ -values from each line to an empirical (ranked order)  $P$ -value distribution. We excluded SNPs with initial minor allele frequencies less than 0.01 from this analysis as uncertainty in the precise allele frequencies

for such rare alleles could have a disproportionate affect on the evidence against neutral evolution. We generated the null correlation matrix for each set of replicate lines using the `GenerateNullData` function with 10,000 replicate draws,  $a = 0.3$ , and  $b = 0.5$ . We then applied the `picmin` function to the empirical  $P$ -values each set of replicate lines (i.e. the five lines for each combination of lineage, generation and host). We applied a false discovery rate (FDR) correction to the `picmin`  $P$ -values to designate SNPs with significant evidence of repeated non-neutral evolution for each treatment group (i.e.  $P < 0.05$  after FDR correction) (Benjamini & Hochberg, 1995).

We then asked whether the same SNPs showed evidence of repeated non-neutral evolution in different pairs of treatment groups (combinations of lineage, generation and host). For this, we identified the 5% of SNPs with the lowest  $P$ -values from `picmin`, regardless of whether these were less than 0.05 after FDR correction (our 5% cutoff is approximately of the same order as the average number of SNPs with significant evidence of repeated evolution in each treatment). Next, for each pair of treatment groups, we computed the overlap between these sets of SNPs, that is, the number of SNPs in the top 5% for pairs of treatment groups. This served as our observed measure of repeated-evolution SNP-sharing between treatments and specifically captured the extent to which SNPs repeatably showing evidence of non-neutral evolution within treatment groups were shared between treatment groups. We generated null expectations for the overlap expected by chance by repeatedly randomizing `picmin`  $P$ -values among SNPs; the randomization procedure preserved information on which SNPs were included in the `picmin` analysis for each treatment group. This was done 1000 times for each treatment group comparison. We used this null distribution to calculate a randomization test  $P$ -value for whether the observed overlap exceeded chance expectations and to calculate the X-fold enrichment of the observed value relative to the null, that is, the ratio of the observed overlap to null expectations, which serves as a quantitative measure of the extent of repeatability between treatments. These analyses were done in R version 4.4 (R Core Team, 2022).

## Results

### Population Growth and Adaptation to Lentil

Despite poor initial survival, 64 out of our 66 experimental lentil lines successfully adapted to this novel, stressful host. The two lines that did not adapt to lentil were BF replicates 6 and 7. The BF lineage showed the slowest cumulative growth rate, while the BF×CA admixed lineage showed the highest (Fig. 2 and Table S1). We also saw a strong incubator effect, with lines 2 through 5, which were housed in the first incubator, experiencing more rapid cumulative growth than populations 6 through 11, which were housed in the second incubator (Fig. 2). Overall, we found that admixture facilitated adaptation to lentil, with higher cumulative growth rates occurring in admixed than non-admixed lineages (Fig. 2 and Table S1).

Results from our Bayesian second-degree polynomial model for cumulative population growth showed a strong signal for evolutionary rescue in all our lentil-adapted lineages. Values of  $\beta_1$  indicate the slope of the cumulative growth curve at time  $t = 0$ . Thus,  $\beta_1$  values can be interpreted as an estimate of the average reproductive rate of each lineage at time  $t = 0$ . The higher the value of  $\beta_1$ , the higher the initial reproductive rate on lentil. The 95% credible intervals for  $\beta_1$  for the BF, BZ, and BF×BZ population all overlapped zero (Table S1). This suggests that at time  $t = 0$ , the reproductive rate (as measured by the average number of adult offspring produced per day) in these populations was not high enough to ensure population persistence on lentil.

Alternatively,  $\beta_1$  values could also be interpreted as a measure of how long it would take for a given founding population of parent beetles to produce enough offspring to fully replace itself, assuming a parental death rate of zero and non-overlapping generations (i.e. generation time). For the CA, BF×CA, and BZ×CA lineages,  $\beta_1$  ranged from 4.7 and 8.6, suggesting that the average reproductive rate at time  $t = 0$  in these lineages was between 4.7 and 8.6 adult offspring per day (see Table S1). At this reproductive rate, it would

hypothetically take between 200 to 500 days for our founding populations of 2000 adult beetles to produce 2000 adult offspring. This, of course, would not be possible in reality as adult seed beetles have limited adult lifespans (less than 10 days) and the majority of first-generation offspring surviving on lentil expected to emerge within 100 days. Thus, even for the three lineages with  $\beta_1$  values credibly greater than zero, the initial reproductive rate estimated by our model was not high enough to suggest that these populations would produce enough offspring to prevent an initial population decline. Our model results for  $\beta_1$  indicate that, on average, all three admixed and all three non-admixed lineages are expected to undergo an initial demographic decline, consistent with the first stage of evolutionary rescue.

The second slope parameter from our Bayesian model,  $\beta_2$ , is a measure of growth rate. A  $\beta_2$  value of zero indicates that population size will remain constant with respect to time (in other words, the population size is stable and no growth occurs), while any value of  $\beta_2$  greater than zero indicates exponential growth, meaning population size will increase with time. A negative value of  $\beta_2$ , meanwhile, indicates that population size will decrease with time. Values of  $\beta_2$  in admixed populations were calculated as the average of  $\beta_2$  values for each parental lineage plus an effect of admixture ( $\beta_2^{AE}$ ).  $\beta_2^{AE}$  values of zero would indicate that the cumulative growth rate in admixed populations was simply the mean of the parental populations' cumulative growth rates. In other words, a  $\beta_2^{AE}$  of zero indicates that the cumulative growth rate of admixed populations falls directly between those of its parents. The effect of admixture for  $\beta_2$  in our linear model was credibly greater than zero for all admixed lineages (Table S1), suggesting that growth rates in all three of our admixed lineages were greater than the average of their parents' growth rates. Notably, values of  $\beta_2$  were credibly greater than zero for all populations, both admixed and non-admixed, indicating that all six populations on average were expected to rebound from their initial demographic decline on lentil.

## Population Structure and Evolutionary Change

Our source cowpea-adapted beetle lineages from Burkina Faso (BF), Brazil (BZ), and California (CA) showed a moderate to strong degree of genetic differentiation from one another. The degree of genetic differentiation between our African population and our two American populations ( $F_{ST}$  for BF and BZ and for BF and CA = 0.20) was twice as high as the degree of differentiation between the two American populations ( $F_{ST}$  for BZ versus CA = 0.09). This result was recapitulated in a PCA (Fig. 3a), with PC1 separating the BF lineage from the BZ and CA lineages, and PC2 separating the BZ and CA lineages. As expected, our three admixed lineages (BF×BZ, BF×CA, and BZ×CA) clustered directly between their two parental populations. One of our lentil-adapted BF lines, BF replicate 5 generation 20, clustered with the BF×BZ admixed lines rather than with the BF purebred lines, indicating that this BF replicate was likely contaminated with BZ beetles at some point during the experiment and underwent admixture. As such, this single BF replicate was removed from all downstream analyses. We observed possible, weaker evidence for contamination of lentil-adapted BF×BZ replicate 2 with CA, but the similarity between BZ and CA makes this less clear and we thus chose to retain this replicate.

Global ancestry estimates also showed clear evidence of admixture consistent with expectations based on their hybrid ancestries (Fig. 3b). Comparison between F7 and F20 generation lentil-adapted hybrids from the BF×BZ and BF×CA lineages showed that global BF ancestry declined over time. While F1 hybrids would have received exactly 50% of their genome from each parental lineage, the mean BF ancestry in F20 admixed lentil lines ranged between 38-45%, a 5-12 percentage point decline in BF ancestry over the course of adaptation to lentil. The F20 admixed cowpea lines, in contrast, showed mean global BF ancestry values between 52-55%. This indicates possible selection against BF ancestry during adaptation to lentil.

Estimates of local ancestry—ancestry block frequencies along chromosomes—also re-

vealed a decline in BF ancestry in lentil-adapted admixed lineages, but not in lineages on cowpea (Figs. 4 and S1–S3). Reduced BF ancestry was especially evident on chromosome 9, and this was especially true for the BF×CA lines (Figs. 4 and S2). In contrast, local ancestry frequencies in lentil and cowpea-adapted BZ×CA lines were ~0.5 across most of the genome. With the exception of lentil-adapted BF×BZ, patterns of local ancestry were similar among replicate lines. For lentil-adapted BF×BZ, BF ancestry was low on most chromosomes in replicates 2 and 3, whereas BF ancestry was only notably reduced on chromosome 9 in replicates 1, 4 and 5 (Fig. S2 and S3).

In addition to the changes in ancestry in admixed populations described above, we documented pervasive, genome-wide evolutionary changes in all populations over the course of this experiment. Mean allele frequency changes (across SNPs and replicates) ranged from 0.046 to 0.072 by generation F7 and 0.051 to 0.094 by generation F20 (Figs. 5, 6 and S4–S6). The biggest changes occurred in lentil-adapted BF, and allele frequency changes were generally larger in lentil-adapted than cowpea-adapted lines. Patterns of allele frequency change varied across the genome. For example, we detected peaks of more pronounced change on chromosome 1 in lentil-adapted BZ, CA, BF×BZ and BZ×CA (Figs. 5 and 6). Similarly, peaks of pronounced allele frequency change were visible on much of chromosome 9 in the lentil-adapted BF×BZ and BZ×CA lineages (Figs. 6 and S5).

Variance effective population sizes ( $N_e$ ) estimated from the F1 to F20 generations varied from a minimum of 38.7 (95% credible interval [CI] 38.0–39.3) in BF replicate 4 on lentil to a maximum of 222.4 (95% CI 216.3–229.2) in BZ×CA replicate 5 on cowpea, consistent with the documented degree of genome-wide allele frequency change (Table S2). All  $N_e$  estimates were considerably lower than the founding population size of the colonies in our experiment (1000 beetles per colony). These estimates varied considerably both across hosts and source populations, but were generally higher for cowpea lines than lentil lines.

## Patterns of Repeated Adaptive Evolution

We found genome-wide evidence of allele frequency change beyond that predicted by the null Wright-Fisher models, with the most pronounced evidence of exceptional evolutionary change often on chromosomes 1 and 9 (Figs. 7, 8, and S7-S9). Wide peaks of non-neutral evolution were especially evident on chromosome 1 in lentil-adapted BZ, CA and BZ×CA and on chromosome 9 in lentil-adapted BF×BZ and BF×CA (Figs. 7 and 8).

In some cases, SNPs showed strong evidence of selection in only a subset of replicate lines (see, for example, the large peak on the right side of chromosome 1 for lentil-adapted BF×BZ, Fig. 8a). Nonetheless, the `picmin` analyses identified hundreds to thousands of SNPs associated with repeated adaptive evolution in each of the treatment groups (Fig. 9a). In general, more SNPs showed significant evidence of repeated, adaptive evolution in lentil-adapted lines than cowpea-adapted lines. The effect of admixture was less clear. Repeatability was highest in the BF×BZ and BF×CA lineages, followed by non-admixed BZ and CA, and then admixed BZ×CA and BF (Fig. 9a). Thus, repeatability was high in admixed lineages that included BF as one of the source lineages but especially low in non-admixed BF (with the caveat that the latter is partially explained by having four rather than five replicates). Finally, in the admixed lineages, repeatability was higher in the F7 generation than in the F20 generation. Fewer than 5% of SNPs exhibited significant ( $P < 0.05$  after FDR correction) evidence of repeated adaptive evolution for most chromosomes and treatment groups, but repeatability was higher for some chromosomes. For example, repeatability was often accentuated in lentil-adapted lines on chromosomes 1 or 9, and in some cases this was even true for cowpea-adapted lines (e.g., chromosome 9 for BF×CA on cowpea) (see Fig. 9b). Interestingly, CA was unique in having a especially high proportion of repeated adaptation SNPs on chromosome 5.

Most pairs of treatment groups and time periods (97 out of 105) showed more evidence of shared, repeated evolution beyond that expected by chance (Table S3, S4 and Fig. 10).

Overall, the highest excess of shared, repeated evolution was found for comparisons involving BF×BZ and BF×CA. For these comparisons, 5.89 to 11.60 times more SNPs than expected were among the top 5% repeated evolution in both treatment groups (or time periods). As expected, the highest overlap was for subsequent time points within the same treatment group (Table S3, S4 and Fig. 10). The effects of admixed versus non-admixed and same versus different host on repeated evolution between treatment groups were more nuanced. Excess overlap was higher between lentil-adapted BF×BZ and BF×CA (8.20 to 10.48×) than between either (ii) cowpea-adapted BF×BZ and BF×CA (7.68 to 8.79×) or (iii) lentil and cowpea-adapted groups from either BF×BZ or BF×CA (6.20 to 8.97×) (Table S3). In contrast, evidence of shared repeated evolution SNPs was weaker between BZ×CA and BF×BZ or BF×CA (1.73–3.81×). We detected notable parallelism between non-admixed BF on lentil and all admixed lineages involving BF (BF×BZ and BF×CA), especially on lentil (5.55 to 5.91×) (Table S3, S4 and Fig. 10), whereas lentil-adapted BZ×CA exhibited greater parallelism with non-admixed BZ and CA on lentil (3.85 to 5.84×).

## Discussion

In this experiment, we assessed patterns of repeated evolution across admixed versus non-admixed seed beetles during adaptation to a novel, stressful host: lentil. We found that admixture facilitated adaptation to lentil, with the BF lineage showing the slowest rate of cumulative population growth during adaptation to this novel host, but evolutionary rescue occurred in almost all lines, and was thus a repeatable evolutionary outcome. Genomic analyses revealed that levels of parallelism varied among lineages in a nuanced way, such that the most SNPs were repeatedly associated with lentil adaptation in the the admixed lineages BF×BZ and BF×CA (>2000), followed by two non-admixed lineages (BZ and CA; ~1800 SNPs), and then the other admixed and non-admixed lineages (BZ×CA and BF; <1000 SNPs). In other words, repeatability was highest in admixed lineages involving BF and non-



admixed lineages excluding BF. SNPs on two chromosomes, 1 and 9, exhibited the highest  
 average levels of evolutionary change and non-neutral evolution in our experiment. We found  
 a large spike of allele frequency change on chromosome 1 in many lineages associated with  
 adaptation to lentil, suggesting that adaptation to this novel host is being driven at least in  
 part by selection on alleles that are adaptive in both admixed and non-admixed lineages. We  
 further found evidence for selection against BF ancestry on chromosome 9 across both hybrid  
 lineages derived from BF parents (BF×BZ and BF×CA), indicating that certain regions  
 of the Burkina Faso genome are likely globally maladaptive on lentil. This same region of  
 chromosome 9 in the non-admixed BF lineage showed moderate evidence of exceptional allele  
 frequency change during adaptation to lentil, again suggesting that certain alleles carried by  
 the BF lineage are globally maladaptive on lentil, regardless of admixture status. Finally,  
 we found a moderate degree of parallelism in evolutionary change between admixed lineages  
 adapted to lentil versus cowpea, suggesting that even under extreme ecological selection, the  
 purging of hybrid incompatibilities still contributes to the degree of evolutionary parallelism  
 observed in admixed lineages. We discuss the implications of these results in greater detail  
 below.

## **Admixture facilitates adaptation to lentil**

Interestingly, it appears that the African lineage (Burkina Faso or BF) showed the poorest  
 capacity to adapt to lentil. The Burkino Faso lineage is from the heart of the purported  
 ancestral range of cowpea seed beetles (Kébé *et al.*, 2017), and as such might be expected to  
 harbor greater genetic diversity than American populations, which were transported across  
 the world via trade and may have undergone significant population bottlenecks during estab-  
 lishment in new locations. Conversely, cowpea is a crop of particular importance in Africa  
 and is widely grown (Kpoviessi *et al.*, 2019), meaning cowpea may have been the only host  
 encountered by the wild Burkina Faso seed beetle population. Cowpea is less widely grown  
 in the Americas, so it is possible that the two American lineages (Brazil and California) had

previous exposure to lentil or to other legume species more commonly grown in these regions, potentially increasing their ability to adapt to novel hosts (but see Messina & Jones, 2009). Alternatively, as all of our lineages have been reared in captivity for many generations, it is possible the Burkina Faso lineage (which was originally collected in 1989; see Messina, 1993) has simply lost some of its original diversity via genetic drift or adaptation to captivity, and its poor adaptive capacity on lentil is simply a reflection of this laboratory history.

It is also possible that other environmental factors alter the adaptive capacity of different lineages of seed beetles on lentil. Despite using very similar models of Percival incubators for this experiment, maintaining the same temperature and day cycle in both, as well as running a dehumidifier full time in both incubators, we nevertheless saw substantial incubator effects across our treatment groups. Replicates 1 through 5 were kept in our first incubator, while replicates 6 through 11 were kept in the second. The first incubator was prone to periods of higher humidity while the second stayed drier during the course of the experiment. Adaptation proceeded much more rapidly in the first incubator (see Fig. 2), and differences in the rate of adaptation across lineages were far less pronounced. Humidity is strongly affected by the total number of colonies in each incubator due to the amount of metabolic water produced by larvae (Bhattacharya *et al.*, 2003), and our incubators were especially prone to humidity spikes during the pupation stage. Humidity has a strong effect on development time and survival in *C. maculatus* (Mainali *et al.*, 2015; Umoetok Akpasam *et al.*, 2017) with the development being the fastest at humidities between 75-80%. Higher humidity appears to increase survival on lentil, suggesting that perhaps differences in adaptive capacity of our parental lineages on lentil could be related to not just the ability to metabolize the novel host, but also their degree of adaptation to low-humidity environments. Further work is warranted to determine how these lineages differ in their survival at various humidity levels, and how the environmental effects of humidity and host interact to affect survival.

## Genetics and repeatability of adaptation to lentil

Numerous SNPs spanning much of chromosomes 1 and 9 were repeatedly associated with adaptation to lentil. These wide and pronounced peaks of association suggest a major role for linkage disequilibrium and linked (indirect) selection in driving patterns of allele frequency change during adaptation. Some of this linkage disequilibrium likely resulted from admixture (Falush *et al.*, 2003), but these patterns of change were not only observed in admixed populations. Thus, these results suggest selection on a few, large regions of reduced recombination, which we hypothesize correspond with large structural variants (i.e. chromosomal rearrangements). Many other recent studies have documented rapid or repeated adaptive evolution in involving structural variation, suggesting this might be a general phenomenon (Todesco *et al.*, 2020; Akopyan *et al.*, 2022; Ma *et al.*, 2024; Nosil *et al.*, 2024; Battlay *et al.*, 2025).

Genomic patterns of adaptation to lentil were similar in the BZ, CA and BZ×CA lineages. The BZ and CA populations are more closely related to each other than either is to BF ( $F_{ST} \sim 0.1$  versus 0.2). Thus, these documented patterns of repeated evolution at the genetic level are consistent with the general pattern that gene reuse during adaptation declines with divergence time or genetic dissimilarity (Conte *et al.*, 2012; Chaturvedi *et al.*, 2022; Bohutínská & Peichel, 2024). Our results also suggest that same alleles can contribute to lentil adaptation in admixed and non-admixed lineages and thus that the effects of these alleles do not necessarily depend strongly on genetic background. Likewise, we found some consistency in adaptation for BF and the admixed lineages BF×BZ and BF×CA, though the contribution of chromosome 9 was more pronounced in the admixed lineages than purebred BF. Moreover, the weaker signal on chromosome 1 for BF suggests that the hypothesized large structural variant on chromosome 1 in BZ and CA might be absent from BF. However, testing this hypothesis requires additional data and analyses (e.g., whole genome comparative alignments) or experiments, especially given the large bottleneck (and associated genome-wide changes) caused by the initial host shift to lentil.

Lastly, we found that the degree of parallelism during adaptation to lentil across replicates in the Brazil (BZ) and California (CA) purebred lineages was higher than the level of parallelism observed in admixed BZ×CA on lentil. This could simply be a byproduct of admixture: if transgressive segregation led to a greater variance in genotypes in admixed populations, then it might be more likely that different genomic backgrounds would survive the severe population bottleneck imposed by adaptation to lentil in different replicates of admixed populations. This could lead to a decrease in the predictability of evolution in admixed lineages during adaptation to extreme environments.

## Hybrid incompatibilities contribute to parallelism

Despite the strong selective pressure imposed by lentil, the overall level of parallelism between cowpea- and lentil-adapted lineages was still reasonably high (3.90 to 8.97× higher than expected by chance). Shared peaks of (non-neutral) allele frequency change between BF×BZ and BF×CA on both lentil and cowpea lineages suggest that there may be hybrid incompatibilities associated with the BF lineage that are shared across hybrid types. Taken together, this evidence suggests that even in the face of strong ecological stress, hybrid incompatibilities may still play a major role in driving evolutionary change in admixed populations. This is consistent with results from other studies on admixed lineages in natural or neutral environments (Matute *et al.*, 2020; Langdon *et al.*, 2022; Kato *et al.*, 2024; Owens *et al.*, 2025).

## Conclusion

In conclusion, we found that admixture facilitated adaptation to lentil, and that adaptation to lentil in cowpea seed beetles is driven in part by selection on globally-adaptive alleles in both admixed and non-admixed lineages. We also found evidence that certain regions of genome from the African lineage (BF) appear to be globally maladaptive on lentil, and

this led to parallel selection against BF ancestry in lentil-adapted lineages across hybrid types. Finally, we saw a moderate degree of parallelism in evolutionary change between admixed lineages adapted to lentil versus cowpea, suggesting that even during evolutionary rescue, the purging of hybrid incompatibilities may still be a major contributor to patterns of evolutionary parallelism observed in admixed lineages.

## Acknowledgments

Thank you to Megan Brady, Angélica Traslaviña, Tara Saley, Daniel Johnson, Camden Treat for their many hours of careful assistance maintaining beetle colonies, collecting population growth data, preparing DNA samples, and providing much-needed company over the years during this very long, often laborious experiment. Special thanks to Dr. Frank Messina, who spent countless hours sharing his extraordinary knowledge of cowpea seed beetles with me, and whose expertise will be sorely missed. Support and resources from the Center for High Performance Computing at the University of Utah are gratefully acknowledged. This work was funded by the National Science Foundation (NSF GRFP awarded to AS, fellow 2017239847; NSF DEB 1844941 to ZG) and the Utah Agricultural Experiment Station (project 1586 to ZG).

## Literature Cited

- Akopyan M, Tigano A, Jacobs A, Wilder AP, Baumann H, Therikildsen NO (2022) Comparative linkage mapping uncovers recombination suppression across massive chromosomal inversions associated with local adaptation in Atlantic silversides. *Molecular Ecology*, **31**, 3323–3341.
- Alexander HK, Martin G, Martin OY, Bonhoeffer S (2014) Evolutionary rescue: linking theory for conservation and medicine. *Evolutionary Applications*, **7**, 1161–1179.

- Angus R, Dellow J, Winder C, Credland P (2011) Karyotype differences among four species of *Callosobruchus* Pic (Coleoptera: Bruchidae). *Journal of Stored Products Research*, **47**, 76–81.
- Arnqvist G, Westerberg I, Galbraith J, *et al.* (2023) A chromosome-level assembly of the seed beetle *Callosobruchus maculatus* genome with annotation of its repetitive elements. *G3 Genes|Genomes|Genetics*, **14**, jkad266.
- Battlay P, Craig S, Putra AR, *et al.* (2025) Rapid parallel adaptation in distinct invasions of *Ambrosia artemisiifolia* is driven by large-effect structural variants. *Molecular Biology and Evolution*, **42**, msae270.
- Benjamini Y, Hochberg Y (1995) Controlling the false discovery rate: a practical and powerful approach to multiple testing. *Journal of the Royal Statistical Society: Series B (Methodological)*, **57**, 289–300.
- Bewick ER, Dyer KA (2014) Reinforcement shapes clines in female mate discrimination in *Drosophila subquinaria*. *Evolution*, **68**, 3082–3094.
- Bhargav VV, Freeland JR, Dorken ME (2022) Evidence of hybrid breakdown among invasive hybrid cattails (*Typha* × *glauca*). *Heredity*, **129**, 195–201.
- Bhattacharya B, Barik A, Banerjee T (2003) Bioenergetics and water balance in *callosobruchus maculatus* (f.)(coleoptera: Bruchidae) larval populations. *Oriental insects*, **37**, 423–437.
- Bohutínská M, Peichel CL (2024) Divergence time shapes gene reuse during repeated adaptation. *Trends in Ecology & Evolution*, **39**, 396–407.
- Booker TR, Yeaman S, Whitlock MC (2023) Using genome scans to identify genes used repeatedly for adaptation. *Evolution*, **77**, 801–811.

- Buerkle CA, Morris RJ, Asmussen MA, Rieseberg LH (2000) The likelihood of homoploid hybrid speciation. *Heredity*, **84**, 441–451.
- Burc E, Girard-Tercieux C, Metz M, *et al.* (2025) Life-history adaptation under climate warming magnifies the agricultural footprint of a cosmopolitan insect pest. *Nature Communications*, **16**, 827.
- Calvo-Baltanás V, Wang J, Chae E (2021) Hybrid incompatibility of the plant immune system: an opposite force to heterosis equilibrating hybrid performances. *Frontiers in Plant Science*, **11**, 576796.
- Chaturvedi S, Gompert Z, Feder JL, *et al.* (2022) Climatic similarity and genomic background shape the extent of parallel adaptation in *Timema* stick insects. *Nature Ecology & Evolution*, **6**, 1952–1964.
- Chaturvedi S, Lucas LK, Buerkle CA, *et al.* (2020) Recent hybrids recapitulate ancient hybrid outcomes. *Nature Communications*, **11**, 2179.
- Chhina AK, Thompson KA, Schluter D (2022) Adaptive divergence and the evolution of hybrid trait mismatch in threespine stickleback. *Evolution Letters*, **6**, 34–45.
- Conte GL, Arnegard ME, Peichel CL, Schluter D (2012) The probability of genetic parallelism and convergence in natural populations. *Proceedings of the Royal Society B: Biological Sciences*, **279**, 5039–5047.
- Credland P, Dick K (1987) Food consumption by larvae of three strains of *Callosobruchus maculatus* (Coleoptera: Bruchidae). *Journal of Stored Products Research*, **23**, 31–40.
- Crow JF (1948) Alternative hypotheses of hybrid vigor. *Genetics*, **33**, 477.
- De Carvalho D, Ingvarsson PK, Joseph J, *et al.* (2010) Admixture facilitates adaptation from standing variation in the European aspen (*Populus tremula* L.), a widespread forest tree. *Molecular Ecology*, **19**, 1638–1650.

- Dobzhansky T (1982) *Genetics and the Origin of Species*. Columbia University Press.
- Dowling DK, Abiega KC, Arnqvist G (2007a) Temperature-specific outcomes of cytoplasmic-nuclear interactions on egg-to-adult development time in seed beetles. *Evolution*, **61**, 194–201.
- Dowling DK, Nowostawski AL, Arnqvist G (2007b) Effects of cytoplasmic genes on sperm viability and sperm morphology in a seed beetle: implications for sperm competition theory? *Journal of Evolutionary Biology*, **20**, 358–368.
- Durkee LF, Olazcuaga L, Szymanski R, Melbourne BA, Hufbauer RA (2023) Genetic mixing facilitates adaptation to a novel environmental constraint. *Ecological Entomology*.
- Edwards CJ, Suchard MA, Lemey P, *et al.* (2011) Ancient hybridization and an irish origin for the modern polar bear matriline. *Current Biology*, **21**, 1251–1258.
- Enard D, Petrov DA (2018) Evidence that rna viruses drove adaptive introgression between neanderthals and modern humans. *Cell*, **175**, 360–371.
- Ewens WJ, Ewens W (2004) *Mathematical Population Genetics: Theoretical Introduction*, vol. 27. Springer.
- Falush D, Stephens M, Pritchard JK (2003) Inference of population structure using multilocus genotype data: linked loci and correlated allele frequencies. *Genetics*, **164**, 1567–1587.
- Gaggiotti OE, Foll M (2010) Quantifying population structure using the F-model. *Molecular Ecology Resources*, **10**, 821–830.
- Gompert Z (2016) A continuous correlated beta process model for genetic ancestry in admixed populations. *PloS ONE*, **11**, e0151047.
- Gompert Z, Buerkle CA (2013) Analyses of genetic ancestry enable key insights for molecular ecology. *Molecular Ecology*, **22**, 5278–5294.



- Gompert Z, Fordyce JA, Forister ML, Shapiro AM, Nice CC (2006) Homoploid hybrid speciation in an extreme habitat. *Science*, **314**, 1923–1925.
- Gompert Z, Lucas LK, Buerkle CA, Forister ML, Fordyce JA, Nice CC (2014) Admixture and the organization of genetic diversity in a butterfly species complex revealed through common and rare genetic variants. *Molecular Ecology*, **23**, 4555–4573.
- Gompert Z, Lucas LK, Nice CC, Fordyce JA, Forister ML, Buerkle CA (2012) Genomic regions with a history of divergent selection affect fitness of hybrids between two butterfly species. *Evolution*, **66**, 2167–2181.
- Gompert Z, Messina FJ (2016) Genomic evidence that resource-based trade-offs limit host-range expansion in a seed beetle. *Evolution*, **70**, 1249–1264.
- Guedes RNC, Smith RH, Guedes NMP (2003) Host suitability, respiration rate and the outcome of larval competition in strains of the cowpea weevil, *Callosobruchus maculatus*. *Physiological Entomology*, **28**, 298–305.
- Harris K, Nielsen R (2016) The genetic cost of neanderthal introgression. *Genetics*, **203**, 881–891.
- Hermansen JS, Sæther SA, Elgvin TO, Borge T, Hjelle E, Sætre GP (2011) Hybrid speciation in sparrows i: phenotypic intermediacy, genetic admixture and barriers to gene flow. *Molecular Ecology*, **20**, 3812–3822.
- Jorde PE, Ryman N (2007) Unbiased estimator for genetic drift and effective population size. *Genetics*, **177**, 927–935.
- Juric I, Aeschbacher S, Coop G (2016) The strength of selection against Neanderthal introgression. *PLoS Genetics*, **12**, e1006340.

- 813 Kato S, Arakaki S, Nagano AJ, Kikuchi K, Hirase S (2024) Genomic landscape of introgres-  
814 sion from the ghost lineage in a gobiid fish uncovers the generality of forces shaping hybrid  
815 genomes. *Molecular Ecology*, **33**, e17216.
- 816 Kéb   K, Alvarez N, Tuda M, *et al.* (2017) Global phylogeography of the insect pest *Calloso-*  
817 *bruchus maculatus* (Coleoptera: Bruchinae) relates to the history of its main host, *Vigna*  
818 *unguiculata*. *Journal of Biogeography*, **44**, 2515–2526.
- 819 Kim BY, Huber CD, Lohmueller KE (2018) Deleterious variation shapes the genomic land-  
820 scape of introgression. *PLoS Genetics*, **14**, e1007741.
- 821 Kpoviessi A, Agbahoungba S, Agoyi EE, Chougourou D, Assogbadjo A, *et al.* (2019) Re-  
822 sistance of cowpea to Cowpea bruchid (*Callosobruchus maculatus* Fab.): Knowledge level  
823 on the genetic advances. *Journal of Plant Breeding and Crop Science*, **11**, 185–195.
- 824 Langdon QK, Groh JS, Aguillon SM, *et al.* (2024) Swordtail fish hybrids reveal that  
825 genome evolution is surprisingly predictable after initial hybridization. *PLoS Biology*, **22**,  
826 e3002742.
- 827 Langdon QK, Powell DL, Kim B, *et al.* (2022) Predictability and parallelism in the contem-  
828 porary evolution of hybrid genomes. *PLoS Genetics*, **18**, e1009914.
- 829 Lewontin RC, Birch L (1966) Hybridization as a source of variation for adaptation to new  
830 environments. *Evolution*, pp. 315–336.
- 831 Li H (2011) A statistical framework for snp calling, mutation discovery, association mapping  
832 and population genetical parameter estimation from sequencing data. *Bioinformatics*, **27**,  
833 2987–2993.
- 834 Li H, Durbin R (2009) Fast and accurate short read alignment with Burrows–Wheeler trans-  
835 form. *Bioinformatics*, **25**, 1754–1760.

- Li H, Handsaker B, Wysoker A, *et al.* (2009) The sequence alignment/map format and samtools. *Bioinformatics*, **25**, 2078–2079.
- Ma LJ, Cao LJ, Chen JC, *et al.* (2024) Rapid and repeated climate adaptation involving chromosome inversions following invasion of an insect. *Molecular Biology and Evolution*, **41**, msae044.
- Mainali BP, Kim HJ, Park CG, *et al.* (2015) Interactive effects of temperature and relative humidity on oviposition and development of *Callosobruchus chinensis* (L.) on azuki bean. *Journal of Stored Products Research*, **63**, 47–50.
- Mallet J (2005) Hybridization as an invasion of the genome. *Trends in Ecology & Evolution*, **20**, 229–237.
- Mallet J (2007) Hybrid speciation. *Nature*, **446**, 279–283.
- Mantel SJ, Sweigart AL (2024) Postzygotic barriers persist despite ongoing introgression in hybridizing *Mimulus* species. *Molecular Ecology*, **33**, e17261.
- Matute DR, Comeault AA, Earley E, *et al.* (2020) Rapid and predictable evolution of admixed populations between two *Drosophila* species pairs. *Genetics*, **214**, 211–230.
- McFarlane SE, Jahner JP, Lindtke D, Buerkle CA, Mandeville EG (2022) Selection leads to remarkable variability in the outcomes of hybridization across replicate hybrid zones. *bioRxiv*, pp. 2022–09.
- Meier JI, Marques DA, Mwaiko S, Wagner CE, Excoffier L, Seehausen O (2017) Ancient hybridization fuels rapid cichlid fish adaptive radiations. *Nature communications*, **8**, 14363.
- Messina FJ (1991) Life-history variation in a seed beetle: adult egg-laying vs. larval competitive ability. *Oecologia*, **85**, 447–455.
- Messina FJ (1993) Heritability and ‘evolvability’ of fitness components in *Callosobruchus maculatus*. *Heredity*, **71**, 623–629.

- Messina FJ, Jones JC (2009) Does rapid adaptation to a poor-quality host by *Callosobruchus maculatus* (F.) cause cross-adaptation to other legume hosts? *Journal of Stored Products Research*, **45**, 215–219.
- Messina FJ, Jones JC, Mendenhall M, Muller A (2009) Genetic modification of host acceptance by a seed beetle, *Callosobruchus maculatus* (Coleoptera: Bruchidae). *Annals of the Entomological Society of America*, **102**, 181–188.
- Messina FJ, Lish AM, Gompert Z (2018) Variable responses to novel hosts by populations of the seed beetle *Callosobruchus maculatus* (Coleoptera: Chrysomelidae: Bruchinae). *Environmental Entomology*, **47**, 1194–1202.
- Messina FJ, Lish AM, Springer A, Gompert Z (2020) Colonization of marginal host plants by seed beetles (Coleoptera: Chrysomelidae): Effects of geographic source and genetic admixture. *Environmental Entomology*, **49**, 938–946.
- Moran BM, Payne C, Langdon Q, Powell DL, Brandvain Y, Schumer M (2021) The genomic consequences of hybridization. *Elife*, **10**, e69016.
- Nanaei HA, Cai Y, Alshawi A, *et al.* (2023) Genomic analysis of indigenous goats in southwest asia reveals evidence of ancient adaptive introgression related to desert climate. *Zoological research*, **44**, 20.
- Nocchi G, Whiting JR, Yeaman S (2024) Repeated global adaptation across plant species. *Proceedings of the National Academy of Sciences*, **121**, e2406832121.
- Nosil P, de Carvalho CF, Villoutreix R, *et al.* (2024) Evolution repeats itself in replicate long-term studies in the wild. *Science Advances*, **10**, eadl3149.
- Nouhaud P, Martin SH, Portinha B, Sousa VC, Kulmuni J (2022) Rapid and predictable genome evolution across three hybrid ant populations. *PLoS Biology*, **20**, e3001914.

- Orr HA (2005) The genetic theory of adaptation: a brief history. *Nature Reviews Genetics*, **6**, 119–127.
- Owens GL, Caseys C, Mitchell N, Hübner S, Whitney KD, Rieseberg LH (2025) Shared selection and genetic architecture drive strikingly repeatable evolution in long-term experimental hybrid populations. *Molecular Biology and Evolution*, p. msaf014.
- Oziolor EM, Reid NM, Yair S, *et al.* (2019) Adaptive introgression enables evolutionary rescue from extreme environmental pollution. *Science*, **364**, 455–457.
- Parchman TL, Gompert Z, Mudge J, Schilkey FD, Benkman CW, Buerkle CA (2012) Genome-wide association genetics of an adaptive trait in lodgepole pine. *Molecular Ecology*, **21**, 2991–3005.
- Pereira RJ, Barreto FS, Burton RS (2014) Ecological novelty by hybridization: experimental evidence for increased thermal tolerance by transgressive segregation in *Tigriopus californicus*. *Evolution*, **68**, 204–215.
- R Core Team (2022) *R: A Language and Environment for Statistical Computing*. R Foundation for Statistical Computing, Vienna, Austria.
- Rêgo A, Messina FJ, Gompert Z (2019) Dynamics of genomic change during evolutionary rescue in the seed beetle *Callosobruchus maculatus*. *Molecular Ecology*, **28**, 2136–2154.
- Rieseberg LH, Archer MA, Wayne RK (1999) Transgressive segregation, adaptation and speciation. *Heredity*, **83**, 363–372.
- Rieseberg LH, Raymond O, Rosenthal DM, *et al.* (2003) Major ecological transitions in wild sunflowers facilitated by hybridization. *Science*, **301**, 1211–1216.
- Rosser N, Seixas F, Queste LM, *et al.* (2024) Hybrid speciation driven by multilocus introgression of ecological traits. *Nature*, **628**, 811–817.

- Rossi M, Hausmann AE, Alcamí P, *et al.* (2024) Adaptive introgression of a visual preference gene. *Science*, **383**, 1368–1373.
- Sankararaman S, Mallick S, Patterson N, Reich D (2016) The combined landscape of Denisovan and Neanderthal ancestry in present-day humans. *Current Biology*, **26**, 1241–1247.
- Schneider CA, Rasband WS, Eliceiri KW (2012) NIH Image to ImageJ: 25 years of image analysis. *Nature Methods*, **9**, 671–675.
- Schumer M, Cui R, Powell DL, Rosenthal GG, Andolfatto P (2016) Ancient hybridization and genomic stabilization in a swordtail fish. *Molecular Ecology*, **25**, 2661–2679.
- Schumer M, Xu C, Powell DL, *et al.* (2018) Natural selection interacts with recombination to shape the evolution of hybrid genomes. *Science*, **360**, 656–660.
- Shastri V, Adams PE, Lindtke D, *et al.* (2021) Model-based genotype and ancestry estimation for potential hybrids with mixed-ploidy. *Molecular Ecology Resources*, **21**, 1434–1451.
- Short AW, Streisfeld MA (2023) Ancient hybridization leads to the repeated evolution of red flowers across a monkeyflower radiation. *Evolution Letters*, **7**, 292–304.
- Soria-Carrasco V, Gompert Z, Comeault AA, *et al.* (2014) Stick insect genomes reveal natural selection’s role in parallel speciation. *Science*, **344**, 738–742.
- Stan Development Team (2022a) RStan: the R interface to Stan. R package version 2.21.5.
- Stan Development Team (2022b) Stan modeling language users guide and reference manual. Version 2.30.
- Stelkens RB, Brockhurst MA, Hurst GD, Greig D (2014) Hybridization facilitates evolutionary rescue. *Evolutionary Applications*, **7**, 1209–1217.
- Sun Y, Lu Z, Zhu X, Ma H (2020) Genomic basis of homoploid hybrid speciation within chestnut trees. *Nature Communications*, **11**, 3375.

- Todesco M, Owens GL, Bercovich N, *et al.* (2020) Massive haplotypes underlie ecotypic differentiation in sunflowers. *Nature*, **584**, 602–607.
- Tran BM, Credland PF (1995) Consequences of inbreeding for the cowpea seed beetle, *Callosobruchus maculatus* (F.)(Coleoptera: Bruchidae). *Biological Journal of the Linnean Society*, **56**, 483–503.
- Tuda M, Kagoshima K, Toquenaga Y, Arnqvist G (2014) Global genetic differentiation in a cosmopolitan pest of stored beans: effects of geography, host-plant usage and anthropogenic factors. *PLoS One*, **9**, e106268.
- Tuda M, Rönn J, Buranapanichpan S, Wasano N, Arnqvist G (2006) Evolutionary diversification of the bean beetle genus *Callosobruchus* (Coleoptera: Bruchidae): traits associated with stored-product pest status. *Molecular Ecology*, **15**, 3541–3551.
- Turissini DA, Matute DR (2017) Fine scale mapping of genomic introgressions within the *Drosophila yakuba* clade. *PLoS Genetics*, **13**, e1006971.
- Umoetok Akpassam SB, Iloba BN, Udo IA (2017) Response of *Callosobruchus maculatus* (F.) to varying temperature and relative humidity under laboratory conditions. *Archives of Phytopathology and Plant Protection*, **50**, 13–23.
- Vedder D, Lens L, Martin CA, *et al.* (2022) Hybridization may aid evolutionary rescue of an endangered east african passerine. *Evolutionary Applications*, **15**, 1177–1188.
- Verhoeven KJ, Macel M, Wolfe LM, Biere A (2011) Population admixture, biological invasions and the balance between local adaptation and inbreeding depression. *Proceedings of the Royal Society B: Biological Sciences*, **278**, 2–8.
- Whiting JR, Booker TR, Rougeux C, *et al.* (2024) The genetic architecture of repeated local adaptation to climate in distantly related plants. *Nature Ecology & Evolution*, **8**, 1933–1947.

## **Data Accessibility and Benefit-Sharing**

### Data Accessibility Statement

Raw sequence reads have been deposited in NCBI's SRA (BioProject PRJNA1232334). Scripts, ecological data and downstream genetic data will be available from Dryad (DOI pending). Current versions of scripts and ecological data are available on **GitHub** for review (<https://github.com/zgompert/CmacAdmix>).

### Benefit-Sharing Statement

Benefits from this research accrue from the sharing of our data and results on public databases as described above.

## **Author Contributions**

AS and ZG designed the research. AS performed the research. AS, BK and ZG analyzed the data. AS and ZG wrote the paper.



965 **Figures**

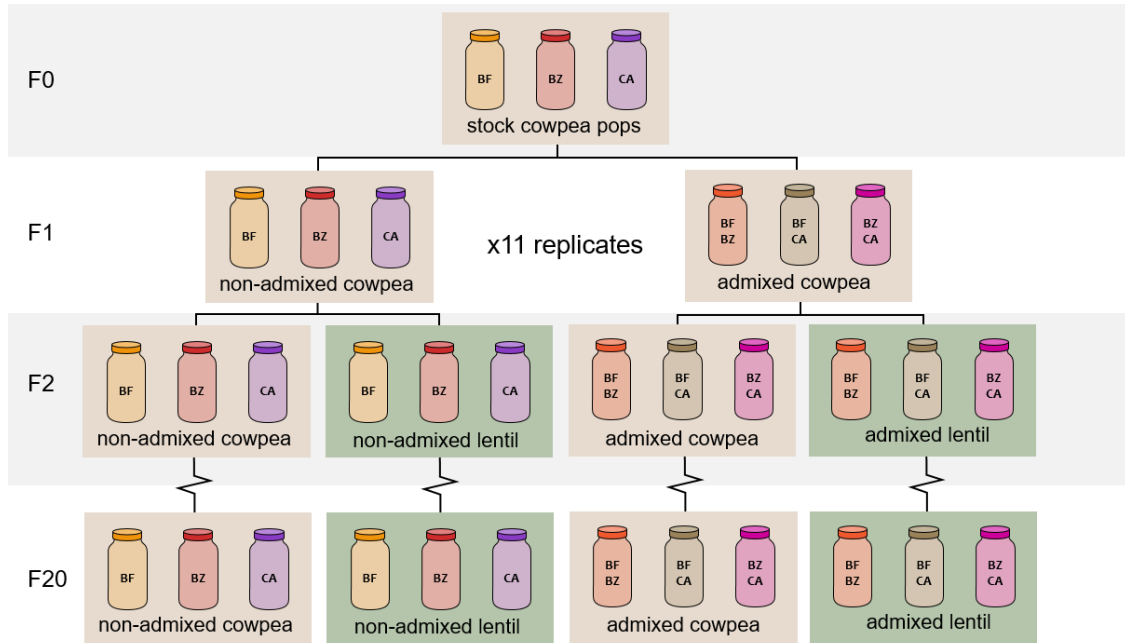


Figure 1: Overview of the experimental design. We evolved 11 replicate lines from each of six lineages—Burkina Faso (BF), Brazil (BZ), California (CA), and the admixed lineages BF×BZ, BF×CA and BZ×CA—on an ancestral host, cowpea, and a novel, stressful host, lentil for 20 generations. We generated DNA sequence data from five replicate lines from each experimental group (lineage and host). Samples were sequenced from the F20 (all lineages) and F7 (only the admixed lineages) generations, along with a single replicate of each of the stock source lineages (BF, BZ and CA).

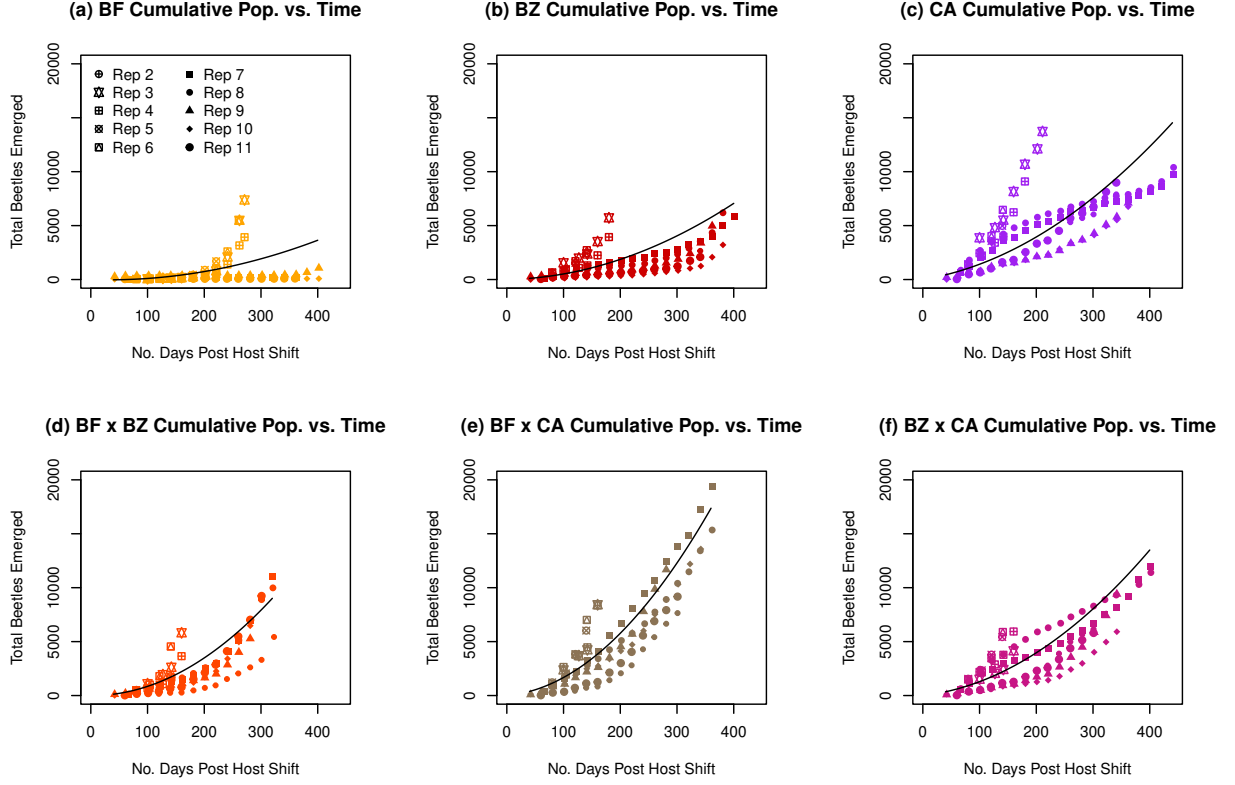


Figure 2: The cumulative number of beetles that emerged from each lentil colony over time by lineage and replicate. Non-admixed lineages are shown in panels (a) through (c), and admixed lineages are shown in panels (d) through (f). Each individual data point represents the total number of beetles produced by a given colony between time  $t = 0$  and time  $t$ , not the population size at time  $t$ . In other words, our plots represent cumulative growth, or the sum of population growth. Thus, a linear relationship between cumulative growth and time would represent a population whose size remains constant with respect to time, while a concave up curve represents population growth over time, and a concave down curve represents a population that is decreasing in size with time. Data points from each individual replicate are represented by point shape. Replicates two through five (hollow point shapes) were all maintained in one incubator, while replicates six through eleven were maintained in a second incubator at the same temperature and day cycle. The average cumulative growth for each lineage fit by our Bayesian model are shown as black curves on each panel.

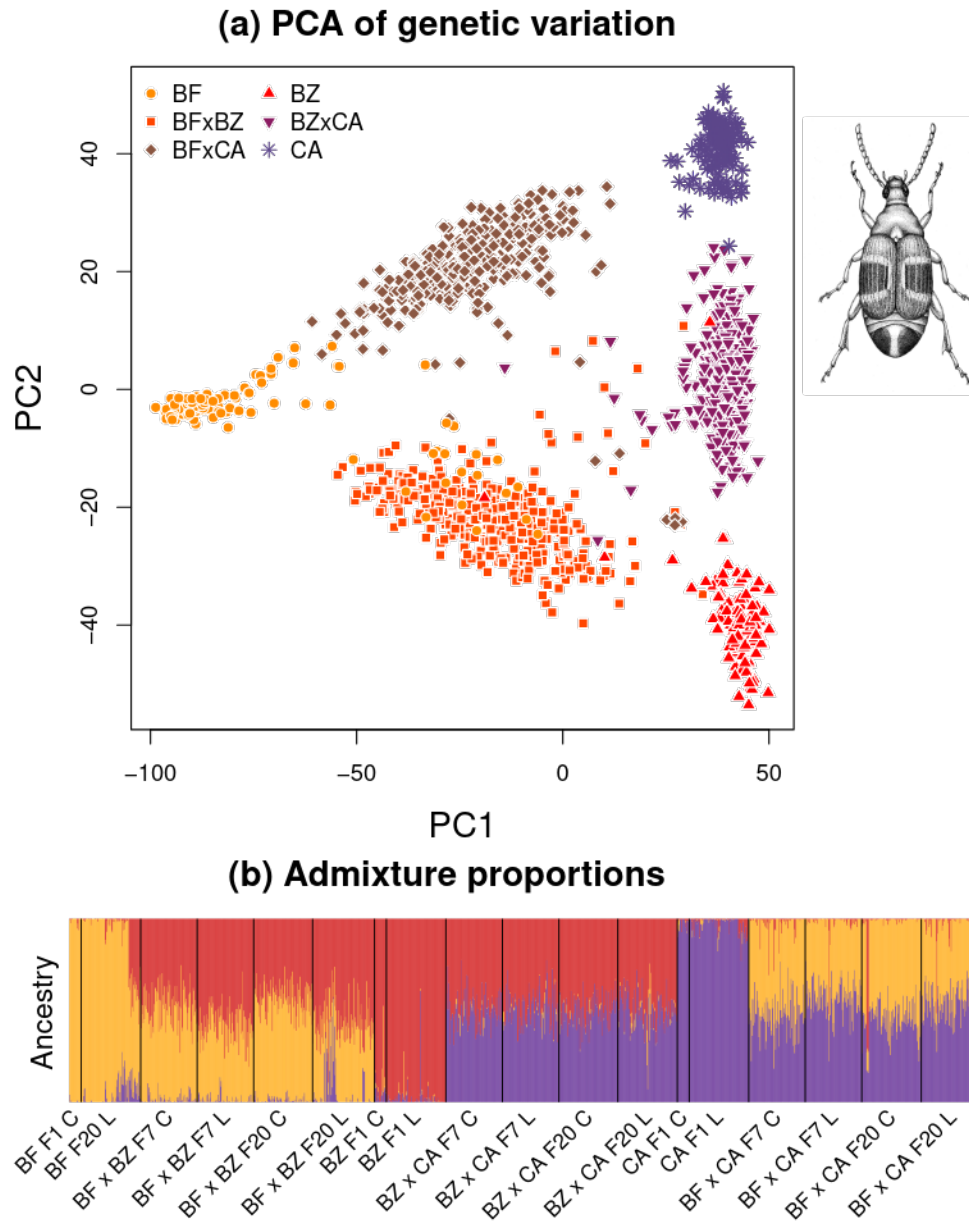


Figure 3: Genetic variation in the experimental *C. maculatus* populations. (a) Principal component analysis of (unscaled) genotype estimates. Each point represents one of the 1536 beetles we sequenced in this study. This includes F7 and F20 generation admixed beetles adapted to both lentil and cowpea from replicates 1 through 5, as well as F1 generation non-admixed beetles adapted to cowpea and F20 generation non-admixed beetles adapted to lentil from replicates 1 through 5. Each unique lineage (BF, BZ, CA, BF $\times$ BZ, BF $\times$ CA, and BZ $\times$ CA) is represented by a unique color $\times$ shape combination on the PCA. (b) Admixture proportions for each individual estimated with **entropy**. Vertical bars represents global ancestry proportions for each of the beetles sequenced. Burkina Faso (BF) ancestry is shown in light orange, Brazil (BZ) ancestry in red, and California (CA) ancestry in purple; C and L denote cowpea-adapted and lentil-adapted lineages, respectively.

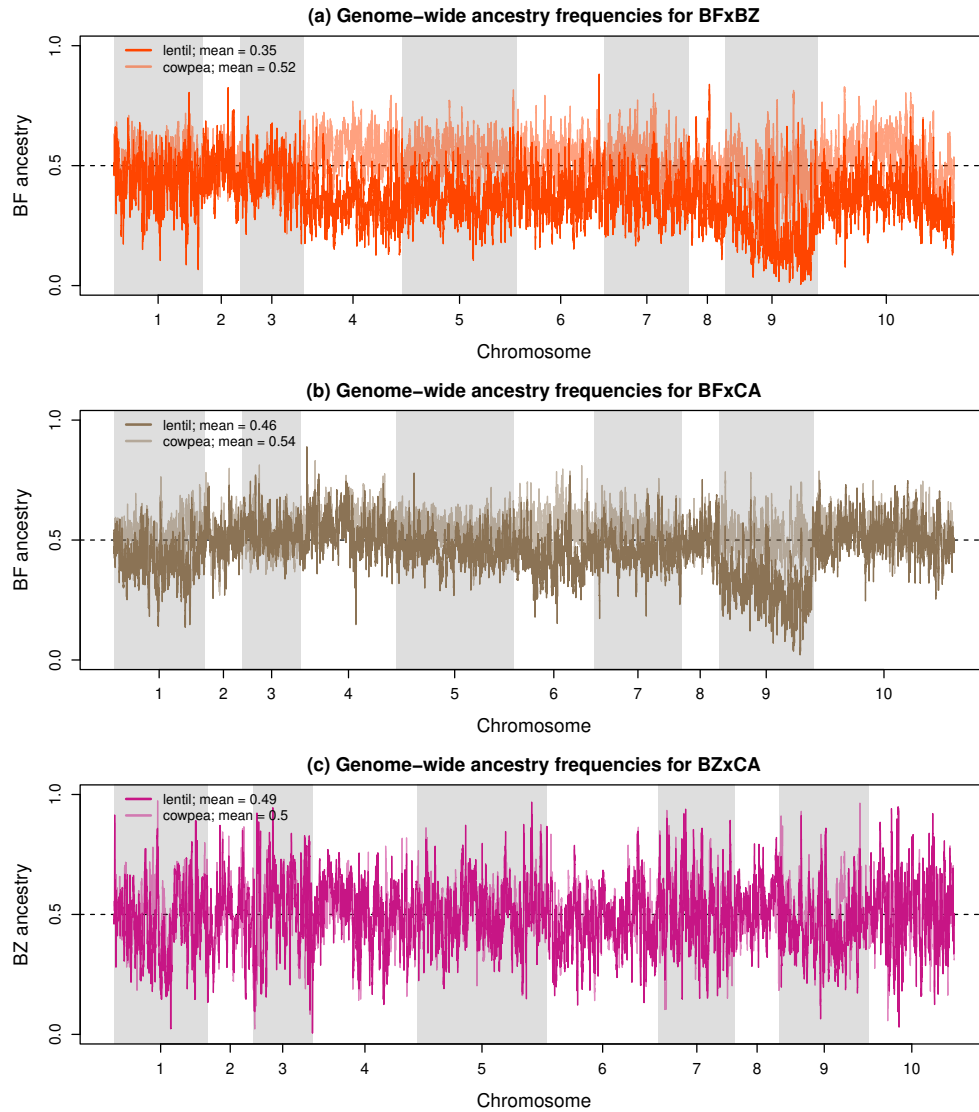


Figure 4: Genome-wide patterns of local ancestry in admixed lineages on lentil. Plots show the frequency of genetic regions inherited from one of two source populations along the genome in the admixed lines at the end of the experiment (20 generations). Lines denote averages across replicate populations with different colors (shades) for the replicate lines on lentil versus cowpea. Genome-average (mean) ancestry frequencies are also reported. Abbreviations used are: BF = Burkina Faso, BZ = Brazil and CA = California.

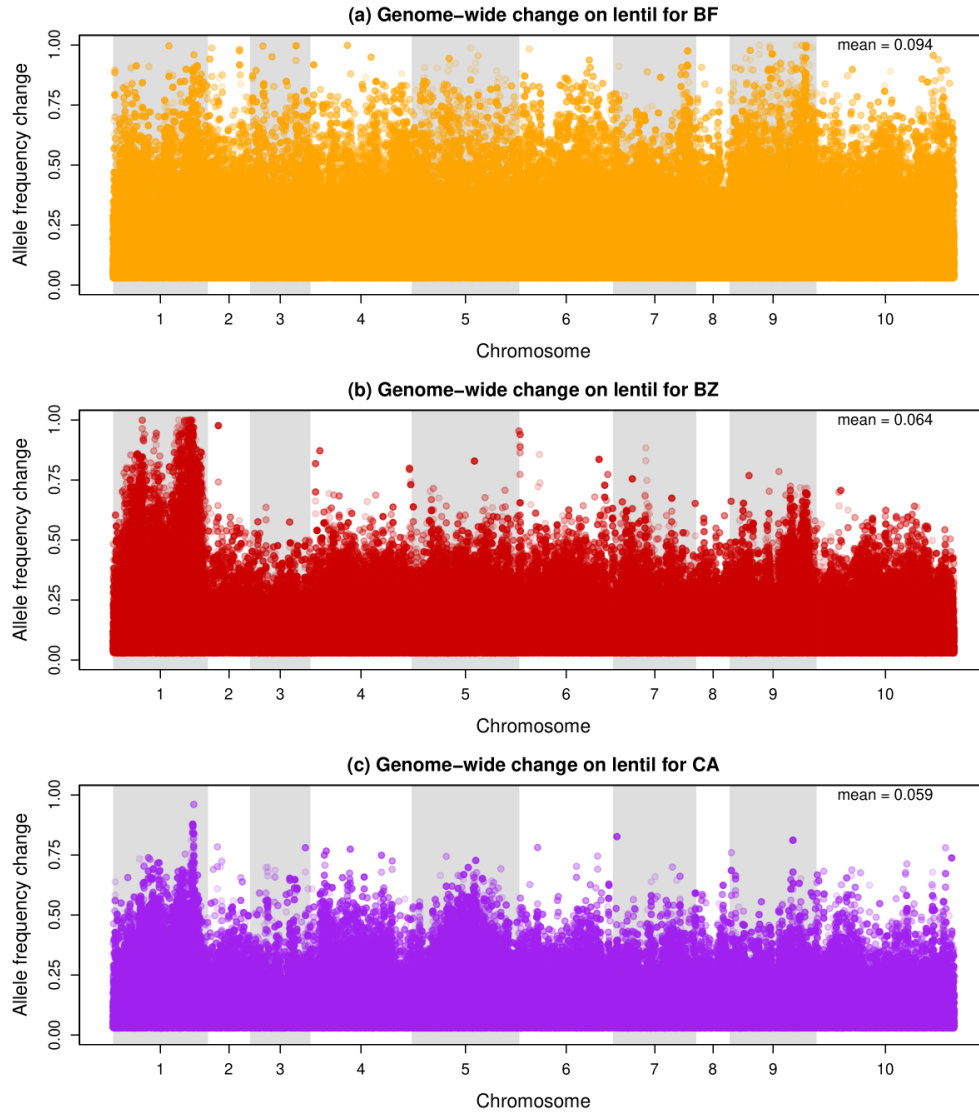


Figure 5: Manhattan plots depicting genome-wide allele frequency change for each of the non-admixed lentil-adapted lines. Results are shown for (a) Burkina Faso = BF, (b) Brazil = BZ, and (c) California = CA at the end of the experiment (after 20 generations). Points denote the unsigned (absolute) allele frequency change for each SNP, arranged in order along the 10 *C. maculatus* chromosomes. Chromosome 10 is the X chromosome. Different color shades are used for each of the five (or four for BF) replicate lines. SNPs with change  $< 0.03$  were omitted from the plot to reduce the file size. The mean change across all SNPs is reported in each panel.

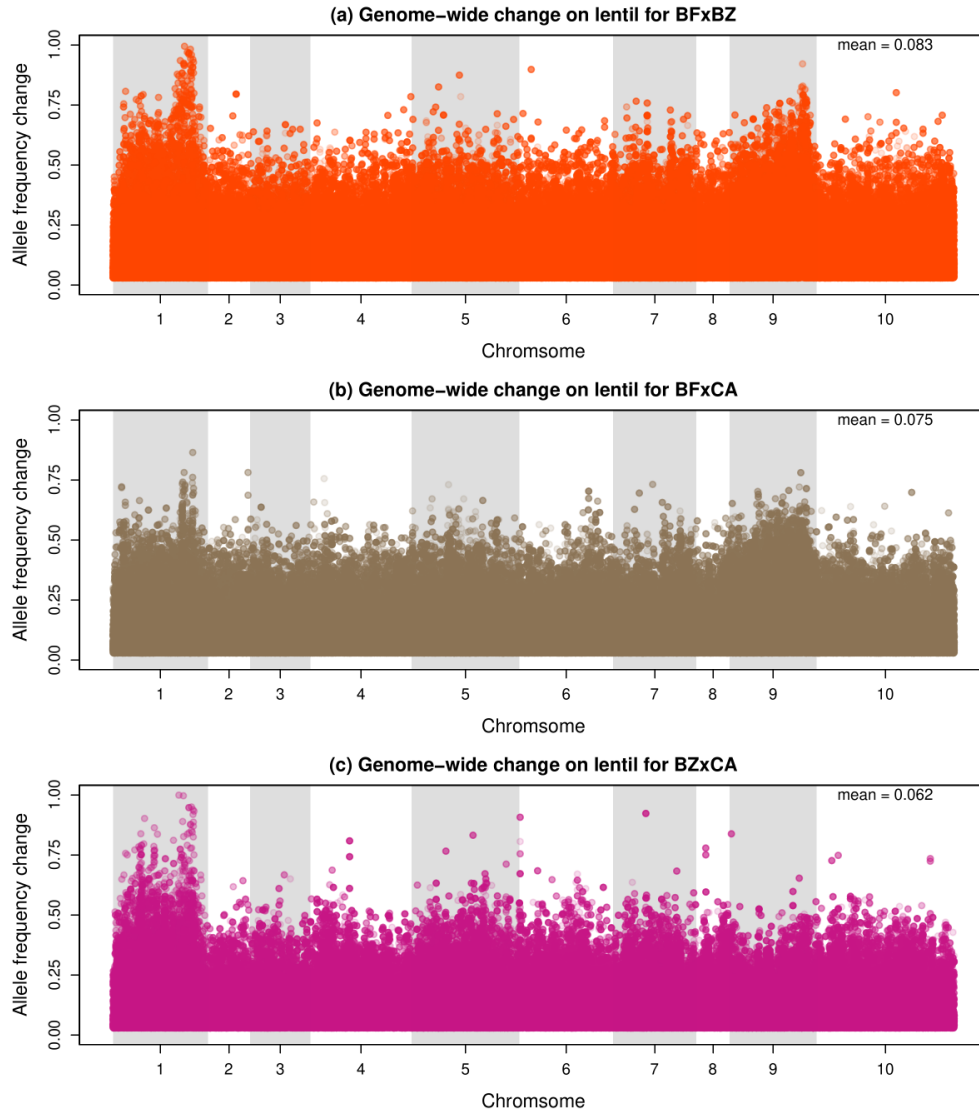


Figure 6: Manhattan plots depicting genome-wide allele frequency change for each of the admixed lentil-adapted lines. Results are shown for (a) Burkina Faso $\times$ Brazil = BF $\times$ BZ, (b) Burkina Faso $\times$ California = BF $\times$ CA, and (c) Brazil $\times$ California = BZ $\times$ CA at the end of the experiment (after 20 generations). Points denote the unsigned (absolute) allele frequency change for each SNP, arranged in order along the 10 *C. maculatus* chromosomes. Chromosome 10 is the X chromosome. Different color shades are used for each of the five (or four for BF) replicate lines. SNPs with change  $< 0.03$  were omitted from the plot to reduce the file size. The mean change across all SNPs is reported in each panel.

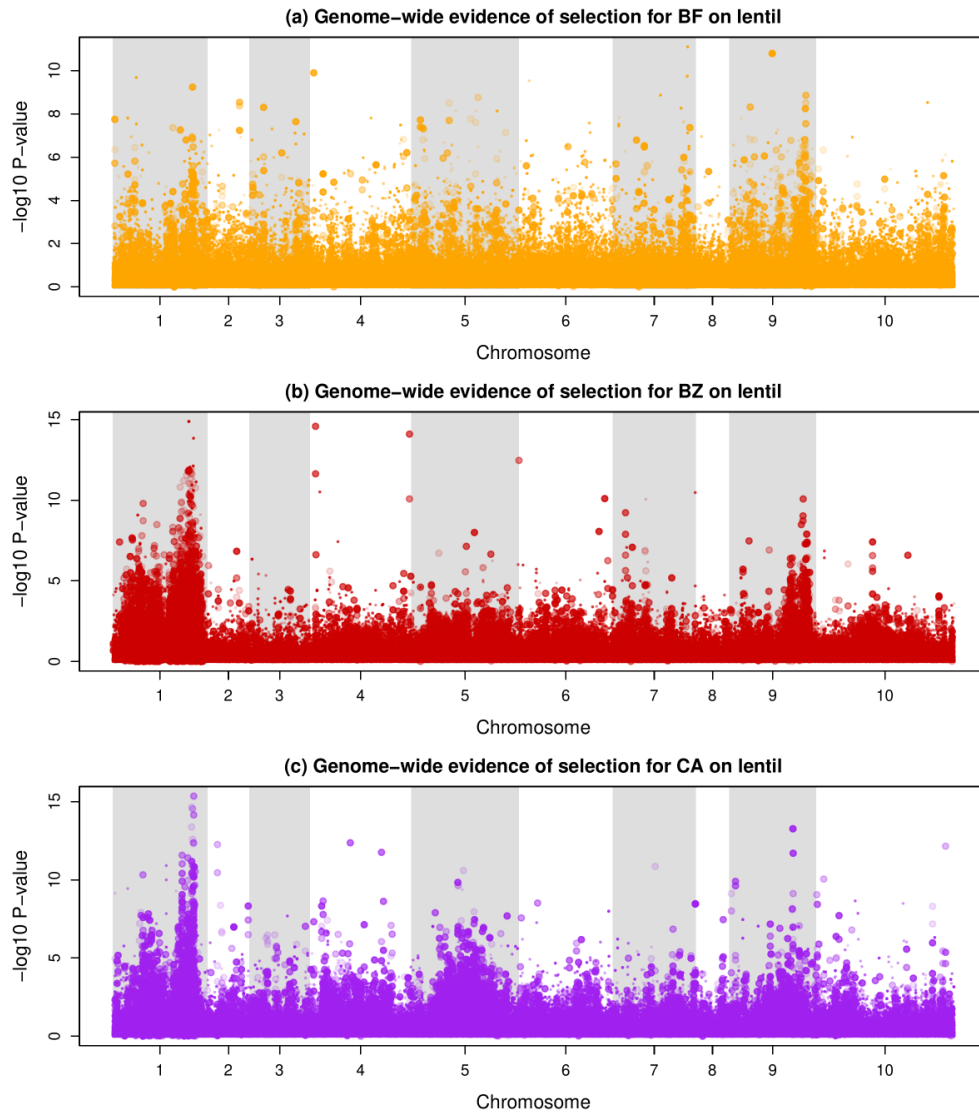


Figure 7: Manhattan plots showing evidence of allele frequency change beyond neutral expectations for each of the non-admixed lentil-adapted lines. Results are shown for (a) Burkina Faso = BF, (b) Brazil = BZ, and (c) California = CA at the end of the experiment (after 20 generations). Points denote  $-\log_{10} P\text{-values}$  from the null Wright-Fisher model for each SNP, with SNPs arranged in order along the 10 *C. maculatus* chromosomes. Chromosome 10 is the X chromosome. Different color shades are used for each of the five (or four for BF) replicate lines. Larger points are used for SNPs with significant evidence of repeated (across replicates) change beyond neutral expectations, that is,  $P\text{-values from } \text{picmin} < 0.05$  following false-discovery rate adjustment.

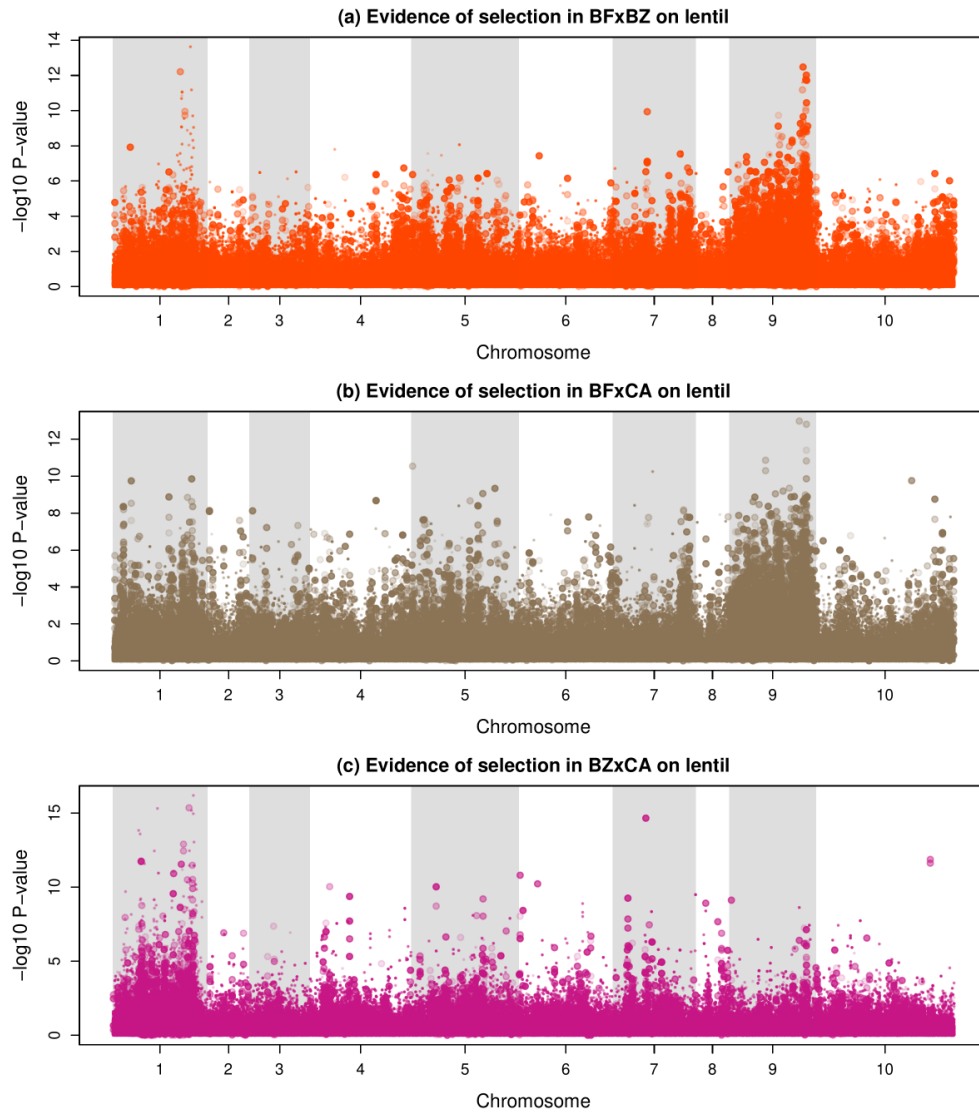


Figure 8: Manhattan plots showing evidence of allele frequency change beyond neutral expectations for each of the admixed lentil-adapted lines. Results are shown for (a) Burkina Faso $\times$ Brazil = BF $\times$ BZ, (b) Burkina Faso $\times$ California = BF $\times$ CA, and (c) Brazil $\times$ California = BZ $\times$ CA at the end of the experiment (after 20 generations). Points denote  $-\log_{10} P$ -values from the null Wright-Fisher model for each SNP, with SNPs arranged in order along the 10 *C. maculatus* chromosomes. Chromosome 10 is the X chromosome. Different color shades are used for each of the five (or four for BF) replicate lines. Larger points are used for SNPs with significant evidence of repeated (across replicates) change beyond neutral expectations, that is,  $P$ -values from `picmin`  $< 0.05$  following false-discovery rate adjustment.



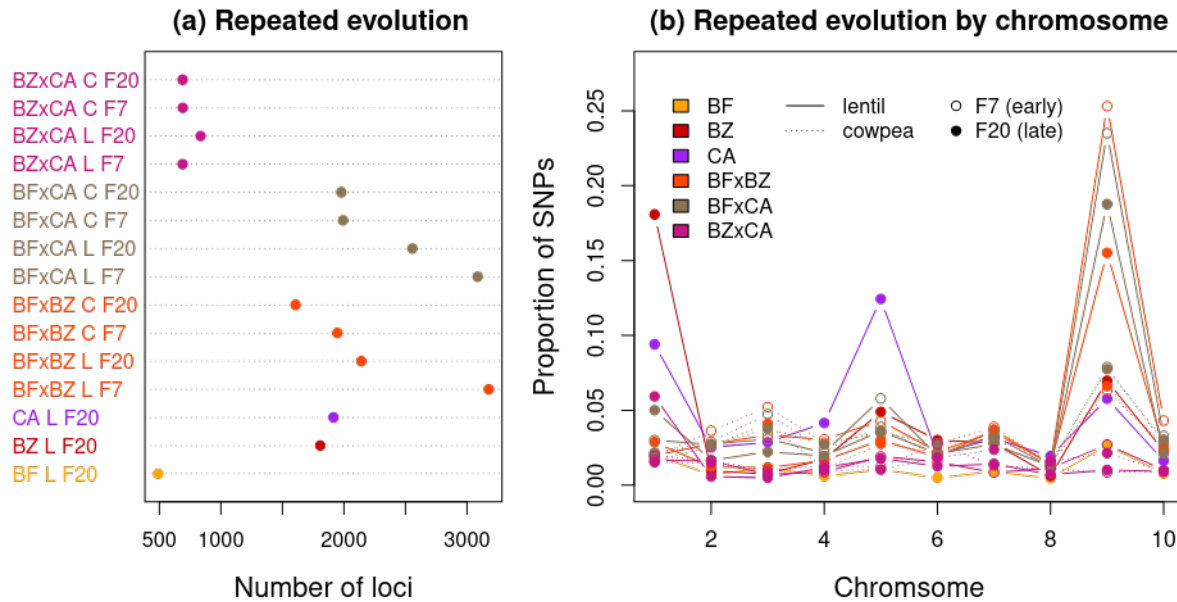


Figure 9: Graphical summary of evidence for repeated evolution among replicates from the same lineage and host treatment. Panel (a) shows the number of SNPs with significant evidence of repeated (across replicates) change beyond neutral expectations (i.e.  $P$ -values from  $\text{picmin} < 0.05$  following false-discovery rate adjustment) for each group. Abbreviations used are: BF = Burkina Faso = BF, BZ = Brazil = BZ, CA = California, C = cowpea, L = lentil, F20 = 20 generations (at the end of the experiment), and F7 = 7 generations (relatively early in the experiment). All results are based on five replicate lines except for BF L (four replicates). Panel (b) summarizes the same  $\text{picmin}$  results for each chromosome. Colored points denote the proportion of SNPs on each chromosome with significant evidence of repeated evolution; colors, point types and line types denote different experimental groups.

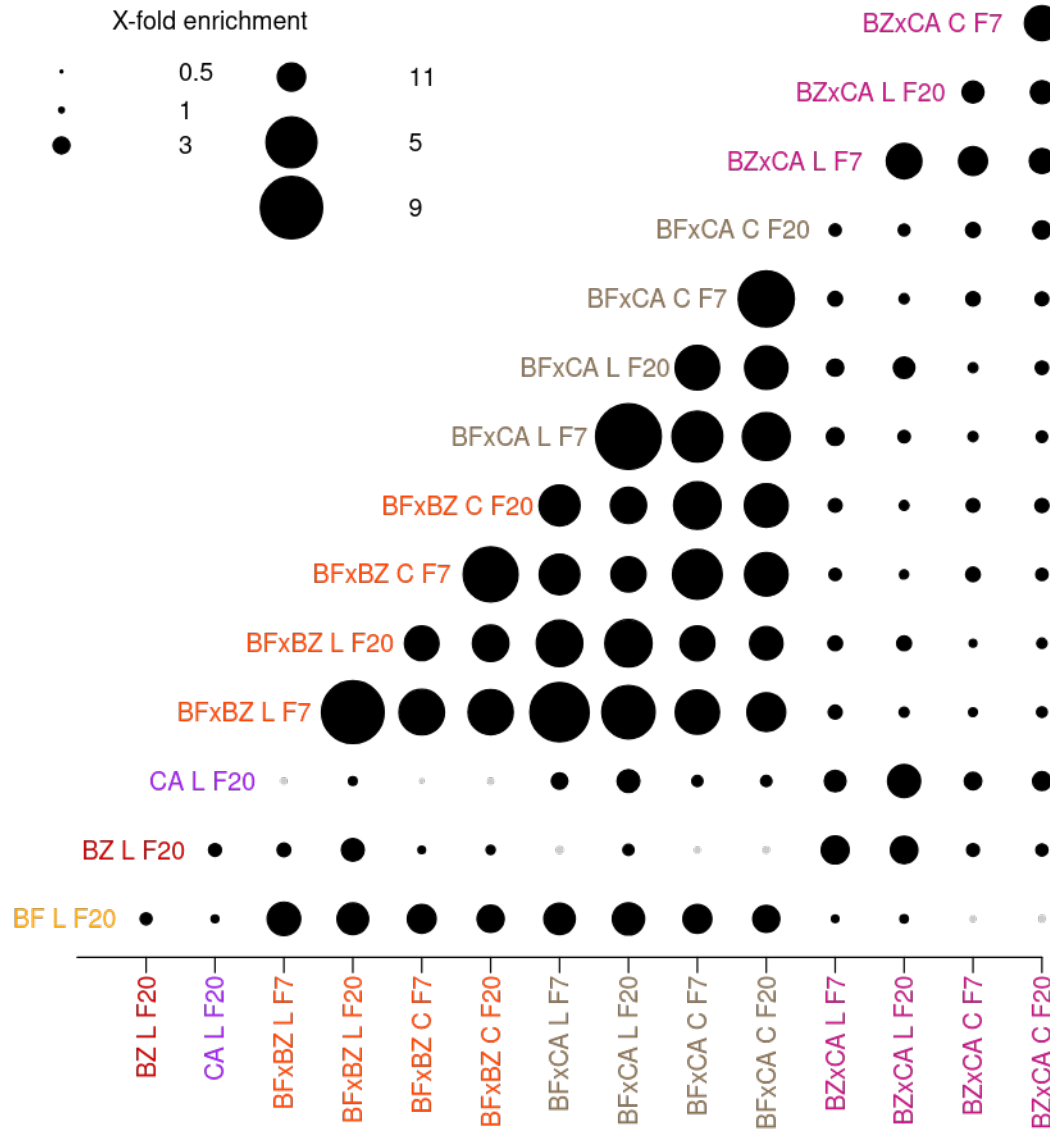


Figure 10: Graphical summary of evidence for repeated evolution between different pairs of experimental groups or time points. Each point denotes the ratio of the observed to expected number of SNPs that were among the top 5% with the strongest evidence of repeated evolution for a pair of experimental groups or time points. Larger points indicate more overlap relative to null expectations of independence between treatments (the null expectation is a 1:1 ratio). Black versus gray circles indicate pairs with ratios that are versus are not significantly greater than 1 with  $P < 0.05$  from a randomization test. Abbreviations used are: BF = Burkina Faso = BF, BZ = Brazil = BZ, CA = California, and C = cowpea, L = lentil.